

# Evidence for an Excess of Soft Photons in Hadronic Decays of $Z^0$

DELPHI Collaboration

## Abstract

Soft photons inside hadronic jets converted in front of the DELPHI main tracker (TPC) in events of  $q\bar{q}$  disintegrations of the  $Z^0$  were studied in the kinematic range  $0.2 < E_\gamma < 1$  GeV and transverse momentum with respect to the closest jet direction  $p_T < 80$  MeV/ $c$ . A clear excess of photons in the experimental data as compared to the Monte Carlo predictions is observed. This excess (uncorrected for the photon detection efficiency) is  $(1.17 \pm 0.06 \pm 0.27) \times 10^{-3} \gamma/jet$  in the specified kinematic region, while the expected level of the inner hadronic bremsstrahlung (which is not included in the Monte Carlo) is  $(0.340 \pm 0.001 \pm 0.038) \times 10^{-3} \gamma/jet$ . The ratio of the excess to the predicted bremsstrahlung rate is then  $(3.4 \pm 0.2 \pm 0.8)$ , which is similar in strength to the anomalous soft photon signal observed in fixed target experiments with hadronic beams.

(Accepted by Eur. Phys. J. C)

J.Abdallah<sup>25</sup>, P.Abreu<sup>22</sup>, W.Adam<sup>51</sup>, P.Adzic<sup>11</sup>, T.Albrecht<sup>17</sup>, T.Alderweireld<sup>2</sup>, R.Aleman-Fernandez<sup>8</sup>, T.Allmendinger<sup>17</sup>, P.P.Allport<sup>23</sup>, U.Amaldi<sup>29</sup>, N.Amapane<sup>45</sup>, S.Amato<sup>48</sup>, E.Anashkin<sup>36</sup>, A.Andreazza<sup>28</sup>, S.Andringa<sup>22</sup>, N.Anjos<sup>22</sup>, P.Antilogus<sup>25</sup>, W-D.Apel<sup>17</sup>, Y.Arnoud<sup>14</sup>, S.Ask<sup>26</sup>, B.Asman<sup>44</sup>, J.E.Augustin<sup>25</sup>, A.Augustinus<sup>8</sup>, P.Baillon<sup>8</sup>, A.Ballestrero<sup>46</sup>, P.Bambade<sup>20</sup>, R.Barbier<sup>27</sup>, D.Bardin<sup>16</sup>, G.J.Barker<sup>17</sup>, A.Baroncelli<sup>39</sup>, M.Battaglia<sup>8</sup>, M.Baillier<sup>25</sup>, K-H.Becks<sup>53</sup>, M.Begalli<sup>6</sup>, A.Behrmann<sup>53</sup>, E.Ben-Haim<sup>20</sup>, N.Benekos<sup>32</sup>, A.Benvenuti<sup>5</sup>, C.Berat<sup>14</sup>, M.Berggren<sup>25</sup>, L.Berntzon<sup>44</sup>, D.Bertrand<sup>2</sup>, M.Besancon<sup>40</sup>, N.Besson<sup>40</sup>, D.Bloch<sup>9</sup>, M.Blom<sup>31</sup>, M.Bluj<sup>52</sup>, M.Bonesini<sup>29</sup>, M.Boonekamp<sup>40</sup>, P.S.L.Booth<sup>†23</sup>, G.Borisov<sup>21</sup>, O.Botner<sup>49</sup>, B.Bouquet<sup>20</sup>, T.J.V.Bowcock<sup>23</sup>, I.Boyko<sup>16</sup>, M.Bracko<sup>43</sup>, R.Brenner<sup>49</sup>, E.Brodet<sup>35</sup>, P.Bruckman<sup>18</sup>, J.M.Brunet<sup>7</sup>, B.Buschbeck<sup>51</sup>, P.Buschmann<sup>53</sup>, M.Calvi<sup>29</sup>, T.Camporesi<sup>8</sup>, V.Canale<sup>38</sup>, F.Carena<sup>8</sup>, N.Castro<sup>22</sup>, F.Cavallo<sup>5</sup>, M.Chapkin<sup>42</sup>, Ph.Charpentier<sup>8</sup>, P.Checchia<sup>36</sup>, R.Chierici<sup>8</sup>, P.Chliapnikov<sup>42</sup>, J.Chudoba<sup>8</sup>, S.U.Chung<sup>8</sup>, K.Cieslik<sup>18</sup>, P.Collins<sup>8</sup>, R.Contri<sup>13</sup>, G.Cosme<sup>20</sup>, F.Cossutti<sup>47</sup>, M.J.Costa<sup>50</sup>, D.Crennell<sup>37</sup>, J.Cuevas<sup>34</sup>, J.D'Hondt<sup>2</sup>, J.Dalmau<sup>44</sup>, T.da Silva<sup>48</sup>, W.Da Silva<sup>25</sup>, G.Della Ricca<sup>47</sup>, A.De Angelis<sup>47</sup>, W.De Boer<sup>17</sup>, C.De Clercq<sup>2</sup>, B.De Lotto<sup>47</sup>, N.De Maria<sup>45</sup>, A.De Min<sup>36</sup>, L.de Paula<sup>48</sup>, L.Di Ciaccio<sup>38</sup>, A.Di Simone<sup>39</sup>, K.Doroba<sup>52</sup>, J.Drees<sup>53,8</sup>, G.Eigen<sup>4</sup>, T.Ekelof<sup>49</sup>, M.Ellert<sup>49</sup>, M.Elsing<sup>8</sup>, M.C.Espirito Santo<sup>22</sup>, G.Fanourakis<sup>11</sup>, D.Fassouliotis<sup>11,3</sup>, M.Feindt<sup>17</sup>, J.Fernandez<sup>41</sup>, A.Ferrer<sup>50</sup>, F.Ferro<sup>13</sup>, U.Flagmeyer<sup>53</sup>, H.Foeth<sup>8</sup>, E.Fokitis<sup>32</sup>, F.Fulda-Quener<sup>20</sup>, J.Fuster<sup>50</sup>, M.Gandelman<sup>48</sup>, C.Garcia<sup>50</sup>, Ph.Gavillet<sup>8</sup>, E.Gaziz<sup>32</sup>, R.Gokieli<sup>8,52</sup>, B.Golob<sup>43</sup>, G.Gomez-Ceballos<sup>41</sup>, P.Goncalves<sup>22</sup>, E.Graziani<sup>39</sup>, G.Grosdidier<sup>20</sup>, K.Grzelak<sup>52</sup>, J.Guy<sup>37</sup>, C.Haag<sup>17</sup>, A.Hallgren<sup>49</sup>, K.Hamacher<sup>53</sup>, K.Hamilton<sup>35</sup>, S.Haug<sup>33</sup>, F.Hauler<sup>17</sup>, V.Hedberg<sup>26</sup>, M.Hennecke<sup>17</sup>, H.Herr<sup>†8</sup>, J.Hoffman<sup>52</sup>, S-O.Holmgren<sup>44</sup>, P.J.Holt<sup>8</sup>, M.A.Houlden<sup>23</sup>, K.Hultqvist<sup>44</sup>, J.N.Jackson<sup>23</sup>, G.Jarlskog<sup>26</sup>, P.Jarry<sup>40</sup>, D.Jeans<sup>35</sup>, E.K.Johansson<sup>44</sup>, P.D.Johansson<sup>44</sup>, P.Jonsson<sup>27</sup>, C.Joram<sup>8</sup>, L.Jungermann<sup>17</sup>, F.Kapusta<sup>25</sup>, S.Katsanevas<sup>27</sup>, E.Katsoufis<sup>32</sup>, G.Kernel<sup>43</sup>, B.P.Kersevan<sup>8,43</sup>, U.Kerzel<sup>17</sup>, B.T.King<sup>23</sup>, N.J.Kjaer<sup>8</sup>, P.Kluit<sup>31</sup>, P.Kokkinias<sup>11</sup>, C.Kourkoumelis<sup>3</sup>, O.Kouznetsov<sup>16</sup>, Z.Krumstein<sup>16</sup>, M.Kucharczyk<sup>18</sup>, J.Lamsa<sup>1</sup>, G.Leder<sup>51</sup>, F.Ledroit<sup>14</sup>, L.Leinonen<sup>44</sup>, R.Leitner<sup>30</sup>, J.Lemonne<sup>2</sup>, V.Lepeltier<sup>20</sup>, T.Lesiak<sup>18</sup>, W.Liebig<sup>53</sup>, D.Liko<sup>51</sup>, A.Lipniacka<sup>44</sup>, J.H.Lopes<sup>48</sup>, J.M.Lopez<sup>34</sup>, D.Loukas<sup>11</sup>, P.Lutz<sup>40</sup>, L.Lyons<sup>35</sup>, J.MacNaughton<sup>51</sup>, A.Malek<sup>53</sup>, S.Maltezos<sup>32</sup>, F.Mandl<sup>51</sup>, J.Marco<sup>41</sup>, R.Marco<sup>41</sup>, B.Marechal<sup>48</sup>, M.Margoni<sup>36</sup>, J-C.Marin<sup>8</sup>, C.Mariotti<sup>8</sup>, A.Markou<sup>11</sup>, C.Martinez-Rivero<sup>41</sup>, J.Masik<sup>12</sup>, N.Mastroiannopoulos<sup>11</sup>, F.Matorras<sup>41</sup>, C.Matteuzzi<sup>29</sup>, F.Mazzucato<sup>36</sup>, M.Mazzucato<sup>36</sup>, R.Mc Nulty<sup>23</sup>, C.Meroni<sup>28</sup>, E.Migliore<sup>45</sup>, W.Mitaroff<sup>51</sup>, U.Mjoernmark<sup>26</sup>, T.Moa<sup>44</sup>, M.Moch<sup>17</sup>, K.Moenig<sup>8,10</sup>, R.Monge<sup>13</sup>, J.Montenegro<sup>31</sup>, D.Moraes<sup>48</sup>, S.Moreno<sup>22</sup>, P.Morettini<sup>13</sup>, U.Mueller<sup>53</sup>, K.Muenich<sup>53</sup>, M.Mulders<sup>31</sup>, L.Mundim<sup>6</sup>, W.Murray<sup>37</sup>, B.Muryn<sup>19</sup>, G.Myatt<sup>35</sup>, T.Myklebust<sup>33</sup>, M.Nassiakou<sup>11</sup>, F.Navarria<sup>5</sup>, K.Nawrocki<sup>52</sup>, R.Nicolaidou<sup>40</sup>, M.Nikolenko<sup>16,9</sup>, A.Oblakowska-Mucha<sup>19</sup>, V.Obratzov<sup>42</sup>, A.Olshevski<sup>16</sup>, A.Onofre<sup>22</sup>, R.Orava<sup>15</sup>, K.Osterberg<sup>15</sup>, A.Ouraou<sup>40</sup>, A.Oyanguren<sup>50</sup>, M.Paganoni<sup>29</sup>, S.Paiano<sup>5</sup>, J.P.Palacios<sup>23</sup>, H.Palka<sup>18</sup>, Th.D.Papadopoulou<sup>32</sup>, L.Pape<sup>8</sup>, C.Parkes<sup>24</sup>, F.Parodi<sup>13</sup>, U.Parzefall<sup>8</sup>, A.Passeri<sup>39</sup>, O.Passon<sup>53</sup>, L.Peralta<sup>22</sup>, V.Perepelitsa<sup>50</sup>, A.Perrotta<sup>5</sup>, A.Petrolini<sup>13</sup>, J.Piedra<sup>41</sup>, L.Pieri<sup>39</sup>, F.Pierre<sup>40</sup>, M.Pimenta<sup>22</sup>, E.Piotto<sup>8</sup>, T.Podobnik<sup>43</sup>, V.Poireau<sup>8</sup>, M.E.Pol<sup>6</sup>, G.Polok<sup>18</sup>, V.Pozdniakov<sup>16</sup>, N.Pukhaeva<sup>2,16</sup>, A.Pullia<sup>29</sup>, J.Rames<sup>12</sup>, A.Read<sup>33</sup>, P.Rebecchi<sup>8</sup>, J.Rehn<sup>17</sup>, D.Reid<sup>31</sup>, R.Reinhardt<sup>53</sup>, P.Renton<sup>35</sup>, F.Richard<sup>20</sup>, J.Ridky<sup>12</sup>, M.Rivero<sup>41</sup>, D.Rodriguez<sup>41</sup>, A.Romero<sup>45</sup>, P.Ronchese<sup>36</sup>, P.Roudeau<sup>20</sup>, T.Rovelli<sup>5</sup>, V.Ruhmann-Kleider<sup>40</sup>, D.Ryabtchikov<sup>42</sup>, A.Sadovsky<sup>16</sup>, L.Salmi<sup>15</sup>, J.Salt<sup>50</sup>, C.Sander<sup>17</sup>, A.Savoy-Navarro<sup>25</sup>, U.Schwickerath<sup>8</sup>, A.Segar<sup>†35</sup>, R.Sekulin<sup>37</sup>, M.Siebel<sup>53</sup>, A.Sisakian<sup>16</sup>, G.Smadja<sup>27</sup>, O.Smirnova<sup>26</sup>, A.Sokolov<sup>42</sup>, A.Sopczak<sup>21</sup>, R.Sosnowski<sup>52</sup>, T.Spaso<sup>8</sup>, M.Stanitzki<sup>17</sup>, A.Stocchi<sup>20</sup>, J.Strauss<sup>51</sup>, B.Stugu<sup>4</sup>, M.Szczekowski<sup>52</sup>, M.Szeptycka<sup>52</sup>, T.Szumlak<sup>19</sup>, T.Tabarelli<sup>29</sup>, A.C.Taffard<sup>23</sup>, F.Tegenfeldt<sup>49</sup>, J.Timmermans<sup>31</sup>, L.Tkatchev<sup>16</sup>, M.Tobin<sup>23</sup>, S.Todorovova<sup>12</sup>, B.Tome<sup>22</sup>, A.Tonazzo<sup>29</sup>, P.Tortosa<sup>50</sup>, P.Travnicek<sup>12</sup>, D.Treille<sup>8</sup>, G.Tristram<sup>7</sup>, M.Trochimczuk<sup>52</sup>, C.Troncon<sup>28</sup>, M-L.Turluer<sup>40</sup>, I.A.Tyapkin<sup>16</sup>, P.Tyapkin<sup>16</sup>, S.Tzamarias<sup>11</sup>, V.Uvarov<sup>42</sup>, G.Valenti<sup>5</sup>, P.Van Dam<sup>31</sup>, J.Van Eldik<sup>8</sup>, N.van Remortel<sup>15</sup>, I.Van Vulpen<sup>8</sup>, G.Vegni<sup>28</sup>, F.Veloso<sup>22</sup>, W.Venus<sup>37</sup>, P.Verdier<sup>27</sup>, V.Verzi<sup>38</sup>, D.Vilanova<sup>40</sup>, L.Vitale<sup>47</sup>, V.Vrba<sup>12</sup>, H.Wahlen<sup>53</sup>, A.J.Washbrook<sup>23</sup>, C.Weiser<sup>17</sup>, D.Wicke<sup>8</sup>, J.Wickens<sup>2</sup>, G.Wilkinson<sup>35</sup>, M.Winter<sup>9</sup>, M.Witek<sup>18</sup>, O.Yushchenko<sup>42</sup>, A.Zalewska<sup>18</sup>, P.Zalewski<sup>52</sup>, D.Zavrtanik<sup>43</sup>, V.Zhuravlov<sup>16</sup>, N.I.Zimin<sup>16</sup>, A.Zintchenko<sup>16</sup>, M.Zupan<sup>11</sup>

- 
- <sup>1</sup>Department of Physics and Astronomy, Iowa State University, Ames IA 50011-3160, USA
- <sup>2</sup>Physics Department, Universiteit Antwerpen, Universiteitsplein 1, B-2610 Antwerpen, Belgium and IIHE, ULB-VUB, Pleinlaan 2, B-1050 Brussels, Belgium and Faculté des Sciences, Univ. de l'Etat Mons, Av. Maistriau 19, B-7000 Mons, Belgium
- <sup>3</sup>Physics Laboratory, University of Athens, Solonos Str. 104, GR-10680 Athens, Greece
- <sup>4</sup>Department of Physics, University of Bergen, Allégaten 55, NO-5007 Bergen, Norway
- <sup>5</sup>Dipartimento di Fisica, Università di Bologna and INFN, Via Irnerio 46, IT-40126 Bologna, Italy
- <sup>6</sup>Centro Brasileiro de Pesquisas Físicas, rua Xavier Sigaud 150, BR-22290 Rio de Janeiro, Brazil and Depto. de Física, Pont. Univ. Católica, C.P. 38071 BR-22453 Rio de Janeiro, Brazil and Inst. de Física, Univ. Estadual do Rio de Janeiro, rua São Francisco Xavier 524, Rio de Janeiro, Brazil
- <sup>7</sup>Collège de France, Lab. de Physique Corpusculaire, IN2P3-CNRS, FR-75231 Paris Cedex 05, France
- <sup>8</sup>CERN, CH-1211 Geneva 23, Switzerland
- <sup>9</sup>Institut de Recherches Subatomiques, IN2P3 - CNRS/ULP - BP20, FR-67037 Strasbourg Cedex, France
- <sup>10</sup>Now at DESY-Zeuthen, Platanenallee 6, D-15735 Zeuthen, Germany
- <sup>11</sup>Institute of Nuclear Physics, N.C.S.R. Demokritos, P.O. Box 60228, GR-15310 Athens, Greece
- <sup>12</sup>FZU, Inst. of Phys. of the C.A.S. High Energy Physics Division, Na Slovance 2, CZ-180 40, Praha 8, Czech Republic
- <sup>13</sup>Dipartimento di Fisica, Università di Genova and INFN, Via Dodecaneso 33, IT-16146 Genova, Italy
- <sup>14</sup>Institut des Sciences Nucléaires, IN2P3-CNRS, Université de Grenoble 1, FR-38026 Grenoble Cedex, France
- <sup>15</sup>Helsinki Institute of Physics and Department of Physical Sciences, P.O. Box 64, FIN-00014 University of Helsinki, Finland
- <sup>16</sup>Joint Institute for Nuclear Research, Dubna, Head Post Office, P.O. Box 79, RU-101 000 Moscow, Russian Federation
- <sup>17</sup>Institut für Experimentelle Kernphysik, Universität Karlsruhe, Postfach 6980, DE-76128 Karlsruhe, Germany
- <sup>18</sup>Institute of Nuclear Physics PAN, Ul. Radzikowskiego 152, PL-31142 Krakow, Poland
- <sup>19</sup>Faculty of Physics and Nuclear Techniques, University of Mining and Metallurgy, PL-30055 Krakow, Poland
- <sup>20</sup>Université de Paris-Sud, Lab. de l'Accélérateur Linéaire, IN2P3-CNRS, Bât. 200, FR-91405 Orsay Cedex, France
- <sup>21</sup>School of Physics and Chemistry, University of Lancaster, Lancaster LA1 4YB, UK
- <sup>22</sup>LIP, IST, FCUL - Av. Elias Garcia, 14-1º, PT-1000 Lisboa Codex, Portugal
- <sup>23</sup>Department of Physics, University of Liverpool, P.O. Box 147, Liverpool L69 3BX, UK
- <sup>24</sup>Dept. of Physics and Astronomy, Kelvin Building, University of Glasgow, Glasgow G12 8QQ
- <sup>25</sup>LPNHE, IN2P3-CNRS, Univ. Paris VI et VII, Tour 33 (RdC), 4 place Jussieu, FR-75252 Paris Cedex 05, France
- <sup>26</sup>Department of Physics, University of Lund, Sölvegatan 14, SE-223 63 Lund, Sweden
- <sup>27</sup>Université Claude Bernard de Lyon, IPNL, IN2P3-CNRS, FR-69622 Villeurbanne Cedex, France
- <sup>28</sup>Dipartimento di Fisica, Università di Milano and INFN-MILANO, Via Celoria 16, IT-20133 Milan, Italy
- <sup>29</sup>Dipartimento di Fisica, Univ. di Milano-Bicocca and INFN-MILANO, Piazza della Scienza 2, IT-20126 Milan, Italy
- <sup>30</sup>IPNP of MFF, Charles Univ., Areal MFF, V Holesovickach 2, CZ-180 00, Praha 8, Czech Republic
- <sup>31</sup>NIKHEF, Postbus 41882, NL-1009 DB Amsterdam, The Netherlands
- <sup>32</sup>National Technical University, Physics Department, Zografou Campus, GR-15773 Athens, Greece
- <sup>33</sup>Physics Department, University of Oslo, Blindern, NO-0316 Oslo, Norway
- <sup>34</sup>Dpto. Física, Univ. Oviedo, Avda. Calvo Sotelo s/n, ES-33007 Oviedo, Spain
- <sup>35</sup>Department of Physics, University of Oxford, Keble Road, Oxford OX1 3RH, UK
- <sup>36</sup>Dipartimento di Fisica, Università di Padova and INFN, Via Marzolo 8, IT-35131 Padua, Italy
- <sup>37</sup>Rutherford Appleton Laboratory, Chilton, Didcot OX11 0QX, UK
- <sup>38</sup>Dipartimento di Fisica, Università di Roma II and INFN, Tor Vergata, IT-00173 Rome, Italy
- <sup>39</sup>Dipartimento di Fisica, Università di Roma III and INFN, Via della Vasca Navale 84, IT-00146 Rome, Italy
- <sup>40</sup>DAPNIA/Service de Physique des Particules, CEA-Saclay, FR-91191 Gif-sur-Yvette Cedex, France
- <sup>41</sup>Instituto de Física de Cantabria (CSIC-UC), Avda. los Castros s/n, ES-39006 Santander, Spain
- <sup>42</sup>Inst. for High Energy Physics, Serpukov P.O. Box 35, Protvino, (Moscow Region), Russian Federation
- <sup>43</sup>J. Stefan Institute, Jamova 39, SI-1000 Ljubljana, Slovenia and Laboratory for Astroparticle Physics, Nova Gorica Polytechnic, Kostanjevska 16a, SI-5000 Nova Gorica, Slovenia, and Department of Physics, University of Ljubljana, SI-1000 Ljubljana, Slovenia
- <sup>44</sup>Fysikum, Stockholm University, Box 6730, SE-113 85 Stockholm, Sweden
- <sup>45</sup>Dipartimento di Fisica Sperimentale, Università di Torino and INFN, Via P. Giuria 1, IT-10125 Turin, Italy
- <sup>46</sup>INFN, Sezione di Torino and Dipartimento di Fisica Teorica, Università di Torino, Via Giuria 1, IT-10125 Turin, Italy
- <sup>47</sup>Dipartimento di Fisica, Università di Trieste and INFN, Via A. Valerio 2, IT-34127 Trieste, Italy and Istituto di Fisica, Università di Udine, IT-33100 Udine, Italy
- <sup>48</sup>Univ. Federal do Rio de Janeiro, C.P. 68528 Cidade Univ., Ilha do Fundão BR-21945-970 Rio de Janeiro, Brazil
- <sup>49</sup>Department of Radiation Sciences, University of Uppsala, P.O. Box 535, SE-751 21 Uppsala, Sweden
- <sup>50</sup>IFIC, Valencia-CSIC, and D.F.A.M.N., U. de Valencia, Avda. Dr. Moliner 50, ES-46100 Burjassot (Valencia), Spain
- <sup>51</sup>Institut für Hochenergiephysik, Österr. Akad. d. Wissensch., Nikolsdorfergasse 18, AT-1050 Vienna, Austria
- <sup>52</sup>Inst. Nuclear Studies and University of Warsaw, Ul. Hoza 69, PL-00681 Warsaw, Poland
- <sup>53</sup>Fachbereich Physik, University of Wuppertal, Postfach 100 127, DE-42097 Wuppertal, Germany
- † deceased

# 1 Introduction

Electromagnetic radiation in the soft photon region arising from interacting hadrons is assumed to be well understood theoretically. In classical papers by Landau and Pomeranchuk [1] and Low [2] it has been shown that the main source of soft photons in hadron reactions is the internal hadronic bremsstrahlung, i.e. the bremsstrahlung radiation from the initial and final hadronic states. Later, Gribov [3] defined quantitatively the meaning of the term *soft photon* as applied to high energy hadron reactions: the transverse momentum,  $p_T$ , of such a photon has to be small as compared to typical values of this variable for secondary particles produced in these reactions, which are 300-400 MeV/c.

The experimental investigation of soft photon production in hadron interactions at high energy started with the bubble chamber experiment [4] at SLAC in which photons from the reaction  $\pi^-p \rightarrow \gamma + X$  at an incident momentum of 10.5 GeV/c were studied. A signal consistent at the 30% probability level with the expectations for the inner hadronic bremsstrahlung was found. The result was considered as a confirmation of theoretical predictions for soft photon production.

However in the next experiment, carried out by the WA27 Collaboration at CERN using the BEBC bubble chamber, a clear soft photon signal in excess of the inner bremsstrahlung prediction was reported for a  $K^+p$  exposure at 70 GeV/c [5]. After subtraction of photons coming from all known hadronic decays the residual signal was found to be similar in shape to bremsstrahlung but larger in size by a factor of about four in the  $p_T$  region below 60 MeV/c. Then results from the CERN experiment NA22 with  $K^+$  and  $\pi^+$  beams on protons at 250 GeV/c also demonstrated an excess of soft photons in a similar kinematic region by a factor of 5 to 7 as compared to bremsstrahlung predictions [6]. Similar effects were found later in the experiment WA83 where a fine-grained forward electromagnetic calorimeter was used to detect photons produced in  $\pi^-p$  interactions at 280 GeV/c [7], and again in the experiment WA91 which also used  $\pi^-p$  interactions at 280 GeV/c, but implemented a different technique for the detection of photons by reconstruction of  $e^+e^-$  pairs from photon conversion in a thin lead sheet placed in front of the OMEGA spectrometer tracker [8].

The situation is less clear with a proton projectile. Experiment E855 at BNL with protons at 18 GeV/c on Be and W targets did not find any signal of direct soft photons at central and slightly backward rapidities, imposing an upper limit for such photons at 2.7 times the hadronic bremsstrahlung [9]. In a similar photon kinematic region, the experiment HELIOS at CERN with proton projectiles at 450 GeV/c on a Be target found a direct soft photon signal compatible with the expected hadronic bremsstrahlung, and derived an upper limit on the presence of additional sources of direct soft photons of about a factor of two relative to the bremsstrahlung [10]. Recently, the signal of direct soft photons at the level of four times the bremsstrahlung predictions was observed at forward rapidities in  $pp$  interactions at 450 GeV/c in the CERN experiment WA102 [11]. Note, in the latter paper a summary of experimental results on direct soft photon observations, including kinematic ranges of particular experiments, is also given<sup>1</sup>

Generalizing the results of the experiments which observed an excess of soft photons, it can be concluded that the photon distributions, studied in the very forward region, were reported to be roughly similar in shape to that expected for the inner hadronic bremsstrahlung calculated from QED, but the observed photon rates were several times larger than expected. Owing to this enhancement factor the observed excess photons were dubbed *anomalous*.

<sup>1</sup>In addition, an excess of soft photons with  $E_\gamma < m_\pi c^2/2$  has been also observed in  $\bar{p}p$  interactions at 32 GeV/c [12], however it was not compared with bremsstrahlung predictions.

Meanwhile various theoretical models [13–33] were suggested, aimed at explaining the effect of anomalous photons by introducing new phenomena into the soft physics of hadronic interactions. Some of them were able to describe some particular features of the experimental data, by interpreting anomalous soft photons as a radiation from a cold quark-gluon plasma [13,17,22], a transient new coherent condition of matter [14,24–26], or as a synchrotron radiation from quarks [27–29] in the stochastic QCD vacuum [34]. However, no model was able to describe the experimental data satisfactorily as a whole, especially in a kinematic range where the effect was most prominent (for a review of the theoretical approaches see [16,22]).

In this situation extending the class of reactions in which the phenomenon of anomalous soft photons is investigated has become of interest. This motivated us to study the reaction

$$e^+e^- \rightarrow Z^0 \rightarrow \textit{hadrons} \quad (1)$$

at LEP1 searching for extra photons in hadronic decays of  $Z^0$  bosons.

Several studies of photon production in hadronic  $Z^0$  decays have been carried out by all the LEP experiments [35–44] including searches for anomalous photon radiation from non-Standard Model sources [35,39,41]. The latter aimed at finding photons emitted by a non-standard source or by quarks before or at the beginning of the fragmentation process. Therefore a signal of rather hard photons well separated from other tracks was searched for. In contrast, the current analysis deals with soft photons deep inside jets, with the aim to separate a signal of soft photons coming from the inner hadronic bremsstrahlung (mainly from the final hadronic states) or from unknown photon sources responsible for the anomalous soft photon radiation seen in hadronic experiments. The photon softness can be characterized in this case by a value of the transverse momentum of a photon with respect to the closest jet. We shall use the term  $p_T$  for this variable throughout this article. The  $p_T$  range chosen to be studied in this work extends from 0 to 80 MeV/ $c$ , while searches for anomalous photons carried out so far in LEP experiments required them to be *hard* and *isolated* ( $E_\gamma > 5$  GeV, in general, and at angles to the closest jet  $> 20^\circ$ ), thus at  $p_T > 1.7$  GeV/ $c$ , i.e. well outside our kinematic region.

This paper is organised as follows. Section 2 provides a description of the apparatus, software, and the experimental method applied. This section also includes a description of selection cuts and data samples. Systematic uncertainties arising from various elements of the analysis method, and their estimates are presented in section 3. Section 4 deals with the calculation of the inner hadronic bremsstrahlung and its systematic errors. In section 5 the main results of the analysis are given, both uncorrected and corrected for the detection efficiency. The results show an excess of soft photons in the real data as compared to the Monte Carlo predictions. Section 6 is devoted to the study of possible systematic biases capable of imitating this excess. Finally, section 7 provides a summary and conclusions.

## 2 Experimental technique and data selection

### 2.1 The DELPHI detector

The DELPHI detector is described in detail elsewhere [45,46]. The following is a brief description of the subdetector units relevant for this analysis. In the DELPHI reference frame the  $Z$  axis is taken along the direction of the  $e^-$  beam. The angle  $\Theta$  is the polar angle defined with respect to the  $Z$ -axis,  $\Phi$  is the azimuthal angle about this axis and  $R$  is the distance from this axis.

The DELPHI barrel tracking system relied on the Vertex Detector (VD), the Inner Detector (ID), the Time Projection Chamber (TPC) and the Outer Detector (OD). The barrel electromagnetic calorimeter, the High density Projection Chamber (HPC) lay immediately outside the tracking detectors. It was used in this analysis for cross-checks only. All these detectors were embedded in a superconducting solenoidal coil providing a uniform magnetic field of 1.23 T, aligned parallel to the beam axis.

The TPC, the principal device used in this analysis, was the main tracker of the DELPHI detector; it covered the angular range from  $20^\circ$  to  $160^\circ$  in  $\Theta$  and extended from 30 cm to 122 cm in R. It provided up to 16 space points for pattern recognition and ionization information extracted from 192 wires.

The HPC covered the angles  $\Theta$  from  $43^\circ$  to  $137^\circ$ . It had eighteen radiation lengths for perpendicular incidence, and its energy resolution was  $\Delta E/E = 0.31/E^{0.44} \oplus 0.027$  where  $E$  is in units of GeV [47]. It had a high granularity and provided a sampling of shower energies from nine layers in depth. The angular precisions for high energy photons were  $\pm 1.0$  mrad in  $\Theta$  and  $\pm 1.7$  mrad in  $\Phi$ .

## 2.2 Software

The principal Monte Carlo (MC) data sets used in this analysis were produced with the JETSET 7.3 PS generator [48] with parameters adjusted according to previous QCD studies [49,50]. For the test of possible systematic biases, two other standard generators: ARIADNE 4.6 [51] and HERWIG 5.8C [52] with parameters adjusted by the DELPHI tuning [50] were also used.

No generation of bremsstrahlung photons from final state hadrons was implemented in the MC generators. On the other hand, the initial state radiation (ISR) and photon radiation from quarks of  $Z^0$  disintegrations were produced using the DYMU3 generator [53] and photon implementation in JETSET [54]. However, as will be shown in section 4, the soft photon rates from these sources are very small as compared to the bremsstrahlung from final state hadrons and therefore need not be considered further.

The generated events were fed into the DELPHI detector simulation program DELSIM [46] in order to produce data which are as close as possible to the real raw data. These data were then treated by the reconstruction and analysis programs in exactly the same way as the real data.

To reconstruct jets, the LUCLUS code [55] with a fixed resolution parameter  $d_{join} = 3$  GeV/c was used. To check the stability of the obtained results, the jet-finding algorithms DURHAM [56] and JADE [57] were also used, both with the resolution parameter  $y_{cut} = 0.01$ . The minimal number of jets in the event was required to be two.

## 2.3 Identification of soft photons

As has already been said, the anomalous soft photon production was observed in hadronic reactions at small  $p_T$  and small polar angles relative to an incident hadronic beam. In  $q\bar{q}$  disintegrations of the  $Z^0$  the corresponding “beam” direction is represented by the direction of the initial  $q$  and/or  $\bar{q}$  and thus the photon angle  $\theta_\gamma$  defined with respect to the parent jet axis is taken as the angular variable in our study, with  $p_T$  being the photon momentum projected onto the plane perpendicular to that axis. The requirement for the kinematic range to correspond to that of hadronic reactions (small  $p_T$ , small  $\theta_\gamma$  angles) prevents the use of the DELPHI electromagnetic calorimeters for the detection of

soft photons due to the strong pile-up of hard photons hitting the calorimeters near the jet axis.

Fortunately for the aim of this analysis, the DELPHI setup contains a significant amount of material in front of the sensitive volume of the DELPHI main tracker, the TPC. About 7% of all photons in the barrel region are converted in front of the tracker. These photons produce in general two reconstructible  $e^+e^-$  tracks in the TPC, giving rise to a clean and well defined photon sample which is used in this analysis.

The energy threshold for the reconstruction of these photons is 0.2 GeV. This, together with the upper cutoff of 1 GeV usually applied in soft photon studies, defined the energy range to be investigated,  $0.2 < E_\gamma < 1$  GeV. Since the study of such photons is not typical in the LEP experiments, we present the characteristics of their detection in detail, starting with a description of the algorithm for the reconstruction of converted photons from tracks detected in the TPC.

A search was made along each TPC track for points where the tangent of its trajectory points directly to the beam spot in the  $R\Phi$  projection. Under the assumption that the opening angle of the electron-positron pair is zero, this point represented a possible photon conversion point at radius  $R$ . All tracks which have had a solution  $R$  that was more than one standard deviation away from the main vertex, as defined by the beam spot, were considered to be conversion candidates. If two oppositely charged conversion candidates were found with compatible conversion point parameters they were linked together to form the converted photon. The following selection criteria were imposed:

- the  $\Phi$  difference between the two conversion points was at most 30 mrad;
- the difference between the polar angles  $\Theta$  of the two tracks was at most 15 mrad;
- at least one of the tracks should have no associated point in front of the reconstructed mean conversion radius.

For the pairs fulfilling these criteria a  $\chi^2$  was calculated from  $\Delta\Theta$ ,  $\Delta\Phi$  and the difference of the reconstructed conversion radii  $\Delta R$  in order to find the best combinations in cases where there were ambiguous associations. A constrained fit was then applied to the electron-positron pair candidate which forced a common conversion point with zero opening angle and collinearity between the momentum sum and the line from the beam spot to the conversion point.

## 2.4 Photon detection efficiency. Resolutions.

The photon detection efficiency, i.e. conversion probability combined with the reconstruction efficiency, was determined with the MC events and tabulated against three variables:  $E_\gamma$ ,  $\Theta_\gamma$ , (the photon polar angle to the beam) and  $\theta_\gamma$  (the photon polar angle to the parent jet axis). The efficiency varies with the energy from zero at 0.2 GeV up to 4 - 6% at 1 GeV, depending on the two other variables. Typical dependences of the efficiency on  $E_\gamma$  and  $\theta_\gamma$  are shown in figs. 1a,b.

The accuracy of the converted photon energy measurement was found to be about  $\pm 1.2\%$  in the given kinematic range. The angular precision of the photon direction reconstruction is presented by figs. 1c,d, in which the distributions of the difference between the generated and reconstructed photon angles  $\Theta_\gamma$  and  $\Phi_\gamma$  are shown. These distributions have a Breit-Wigner shape, as expected for the superposition of many Gaussian distributions of varying width [58]. The full widths ( $\Gamma$ 's) of the  $\Delta\Theta_\gamma$  and  $\Delta\Phi_\gamma$  distributions are 4 and 5 mrad, respectively.

The importance of good angular resolution in studying anomalous soft photons was shown in the hadronic beam experiment studies where most of the anomalous soft photons

were observed inside a cone of 10–20 mrad around the beam direction [8,11]. In those experiments the angular accuracy was determined by the precision of the measurement of the photon polar angle  $\theta_\gamma$ , which varied between 1 to 6 mrad (while the accuracy of the beam direction measurement was about 0.1 mrad).

In hadronic decays of  $Z^0$  bosons the accuracy of the measurement of the angle between the initial quark direction and the emitted photon is determined mainly by the angular accuracy of the reconstruction of the former, represented by the jet axis. Typical values of this accuracy in two-jet  $e^+e^-$  annihilation events were reported to be between 50 and 60 mrad [59], depending slightly on the jet-finding algorithm (with best results coming from the LUCLUS code). These results were tested with DELPHI MC events and a similar accuracy was found for the initial quark direction reconstruction. Namely, the mean deviation of the reconstructed jet axis from the primary quark direction for jets of momenta  $> 40$  GeV/ $c$  was found to be about 40 mrad, as can be deduced from the distribution illustrated by fig. 1e, and increases up to 50 mrad for smaller jet momenta. This is much worse than the corresponding accuracy of hadronic beam experiments. The accuracy does not improve by selecting “good events” with small missing energy and/or small missing longitudinal and transverse momenta. A rather moderate improvement of the accuracy (to 25 - 30 mrad) can be achieved by selecting two-jet events with the jet acollinearity smaller than 20 mrad, at the price of a loss of 80% of the two-jet event statistics. No such selections were implemented in this analysis.

Thus the available accuracy of the determination of the initial quark direction in this analysis is expected to spread the angular,  $p_T$ , and (most prominently)  $p_T^2$  distributions of the possible anomalous soft photon signal as compared to the experiments with hadronic beams.

## 2.5 Selection cuts and data samples

Events involving the hadronic decays of the  $Z^0$  from the DELPHI data of the 1992 to 1995 running periods were used in this analysis.

Selection of the hadronic events was based on large charged multiplicity ( $N_{ch} \geq 5$ ) and high visible energy ( $E_{vis} \geq 0.2E_{cm}$ ). In addition, the condition  $30^\circ \leq \Theta_{thrust} \leq 150^\circ$  was imposed, where  $\Theta_{thrust}$  is the angle between the thrust axis and the beam direction. These criteria correspond to an efficiency of  $(85.2 \pm 0.2)\%$  with a  $Z^0 \rightarrow \tau^+\tau^-$  contamination of  $(0.4 \pm 0.1)\%$ .

A total of 3,498,655 events of real data (RD) was selected under these cuts and confronted with  $8 \times 10^6$  MC events selected under the same criteria and properly distributed over all the running periods.

Jets were reconstructed using the detected charged and neutral particles of the event, the charged particles being selected under the following criteria:

- $p > 400$  MeV/ $c$ ;
- $\Delta p/p < 100\%$ ;
- $20^\circ \leq \Theta \leq 160^\circ$ ;
- track length  $> 30$  cm;
- impact parameters below 4 and 10 cm in the  $R\Phi$  and  $Z$  projections, respectively.

The neutral particles were taken within the geometrical acceptances of the subdetectors in which they were reconstructed, within the selection criteria of the appropriate subdetector pattern recognition codes [45,46], without additional cuts.

The selection of jets (whatever jet reconstruction algorithm, LUCLUS, DURHAM, or JADE having been used) was made with the following cuts:



- $30^\circ \leq \Theta_{jet} \leq 150^\circ$ ;
- $P_{jet} \geq 5 \text{ GeV}/c$ ;
- no identified electrons (positrons) were allowed in the jets (electron identification with a standard DELPHI tag);
- if the jet charged multiplicity  $N_{ch} = 1$ , the charged particle must be identified to be not an electron/positron (which is a stronger cut than the rejection of a particle identified as an electron/positron).

The selection of converted photons was made with the following cuts:

- only converted photons with both  $e^+, e^-$  arms reconstructed were considered;
- $20^\circ \leq \Theta_\gamma \leq 160^\circ$ ;
- $5 \text{ cm} \leq R_{conv} \leq 50 \text{ cm}$ , where  $R_{conv}$  is the conversion radius;
- $200 \text{ MeV} \leq E_\gamma \leq 1 \text{ GeV}$ .

A total of 682,364 converted photons was selected under these cuts in the RD and 1,521,030 converted photons in the MC.

### 3 Systematic biases and their uncertainties

In view of the worsening of the signal detectability mentioned in section 2.4, the quality of the MC data becomes important and a highly accurate simulation of the experimental conditions in the MC stream, i.e. minimization of systematic effects biasing the MC distributions with respect to the RD ones, is paramount. Systematic effects due to this bias in the MC data are classified into two types: “software” and “hardware” systematics.

The software systematics are related to an improper reproduction of experimental spectra of photons and charged particles by the MC event generator. The former affects directly the MC produced photon distributions, while the latter does this indirectly by biasing the reconstructed jet direction. Similar bias can be induced by a jet-finding algorithm. Estimates for systematic uncertainties of this type are given in section 3.2.

The hardware systematics are related to biases in the simulation of experimental conditions in the MC stream, i.e. those which appear when transporting MC photons through the DELPHI setup and reconstructing them (after conversion in the DELPHI setup material) from hits simulated in the TPC. These features have been extensively studied throughout all the LEP1 period, with necessary corrections being introduced to the MC code. Some details of this study can be found in papers [47,60]. However, in this analysis an additional procedure was implemented to improve the simulation of experimental conditions in the MC data, called “recalibration”.

#### 3.1 Reduction of hardware systematic bias

The idea was to use wide angle photons ( $\theta_\gamma > 200 \text{ mrad}$ ), for which no signal of anomalous soft photons is expected, to re-normalize the material distribution along the photon path in the simulation, and to account for possible differences in reconstruction of converted photons from the TPC hits along  $e^+e^-$  tracks in the MC and RD. Two types of recalibration were applied. In the first one the wide angle soft photons from the MC and RD samples were collected into two-dimensional distributions, conversion radius  $R_{conv}$  versus the photon polar angle relative to the beam axis,  $\Theta_\gamma$ . For the second type of recalibration the photons were binned according to  $E_\gamma$ . Bin widths of the calibration distributions were varied by factors up to 4 in order to check the stability of the procedure

relative to the binning. The distributions, normalized to an equal number of jets passing the selection criteria, were used to obtain correction coefficients in appropriate bins of the above variables. The corrections were then applied to the MC data.

Both recalibration procedures were tried and have been found to give similar results for the photon rates integrated over the variables used, agreeing within the systematic errors discussed in the next paragraph (see also section 6.4). The results were stable relative to the change of the jet-finding algorithm (LUCLUS, DURHAM or JADE codes). On the other hand, the calibration coefficients varied over LEP1 running periods due to changes in the DELPHI detector, i.e. changes of material distribution in front of the TPC, e.g. due to upgrade of the VD, etc., which required them to be found and used individually for each of the running periods.

To illustrate the quality of the data after recalibration, the distribution of the wide angle,  $0.2 < E_\gamma < 1$  GeV photons against the photon polar angle with respect to the beam direction,  $\Theta_\gamma$ , is displayed in fig. 2. The part of the MC data statistically independent from those involved in the calculation of the recalibration coefficients is used for this, being properly distributed over the data-taking periods considered. The averaged integral difference between the MC and RD in this plot is below 0.9% (with an excess in MC). Expressed in the rate of photons having  $p_T < 80$  MeV/c (the  $p_T$  range under study) which is  $18.4 \times 10^{-3} \gamma/\text{jet}$ , the difference is below  $0.16 \times 10^{-3} \gamma/\text{jet}$ . This value is used as an estimate of the systematic errors of hardware origin in the MC data. It is quoted in table 1 together with other systematic error estimates considered below.

### 3.2 Estimation of software systematic errors

The largest contribution to the software systematic error was found to come from the uncertainty for deviations of the MC spectra produced with the event generator JETSET 7.3 PS, implemented to obtain the principal MC data sets used in this analysis, from the correct distributions of photons in the selected kinematic range,  $0.2 < E_\gamma < 1$  GeV,  $p_T < 80$  MeV/c. These deviations could happen either due to an improper description of the QCD processes in this kinematic range by the model used in the generator (string fragmentation model, [48]), or due to an inadequate representation of the full set of unstable hadrons decaying radiatively at the final stage of the hadronization mechanism.

The systematic errors due to the JETSET generator model and its tuning were estimated in two steps. First, the MC data were used with three different tunings described in [49,50]. In particular, the invariant mass cutoff of parton showers  $Q_0$ , below which partons are not assumed to radiate gluons, and which is important in the soft kinematic region, was varied between 1.73 and 2.25 GeV/c<sup>2</sup> (other parameters correlated with this also being varied in order to keep the overall description of the data as good as possible)<sup>2</sup>. Comparing the photon spectra in our kinematic region for all the three tunings, it was found that the integral photon rates vary within  $\pm 0.4\%$  which can be used as an estimate of the systematic error due to generator tuning. Expressed in photon rates, the difference is at the level of  $0.08 \times 10^{-3} \gamma/\text{jet}$ .

Then the MC data produced with other commonly used MC generators, ARIADNE and HERWIG were studied. The description of a parton shower by ARIADNE is based on color dipoles [51,61], and that of HERWIG on the coherent parton branching mechanism [52]. Unlike the results for high energy isolated photons reported in [37,39,44], no big difference between the JETSET and ARIADNE generators was found in the kinematic range studied in this work. As will be shown below (section 6.2), a systematic uncertainty

<sup>2</sup>At generator level, the stability of the soft photon rate was tested in a wider range of the  $Q_0$ , from 0.3 to 2.25 GeV/c<sup>2</sup>.

due to the generator model for the rate of soft photons of  $p_T < 80$  MeV/ $c$  can be estimated to be at the level of  $0.18 \times 10^{-3} \gamma/\text{jet}$ . Combining this value with the uncertainty due to the tuning, the systematic error due to the event generator was estimated to be  $0.20 \times 10^{-3} \gamma/\text{jet}$ . This value is quoted in table 1.

A sensitive cross-check of the generator model systematics, making use of charged particle spectra (see section 6.5), has shown that the possible systematic bias of this type is likely to be much less than the quoted errors. Another cross-check, based on the comparison of the  $\pi^0$  production in the MC and RD (see section 6.6) involving both the generator and hardware systematics, also demonstrated results in a good agreement with the estimations above. The cross-checks indicate some overestimation of the systematic errors due to the generator model quoted above, nevertheless they are retained.

The next systematic effect to be considered may originate from the possible inadequate representation of unstable hadrons decaying radiatively (other than  $\pi^0$ 's) in the MC code, biasing the MC hadron outcome as compared to the RD. Its study is described in detail in section 6.7. It follows from this study that the value of a systematic error due to effects of this type is at the level of  $0.05 \times 10^{-3} \gamma/\text{jet}$ .

In order to determine the scale of a possible variation of results due to an implementation of a jet-finding algorithm other than LUCCLUS, the DURHAM and JADE algorithms were also used in the analysis (see section 5.1). From the variations obtained the systematic error due to the jet finder was derived to be at the level of  $0.07 \times 10^{-3} \gamma/\text{jet}$ .

Since the results of this work are presented both uncorrected and corrected for the detection efficiency, in the latter case the systematic errors resulting from the correction have to be taken into account. The integral systematic error due to the efficiency correction in the photon  $p_T$  range below 80 MeV/ $c$  was found to be 6% of the corrected photon rates (both, for the RD and for the MC, as well as for their difference). This error has two components. The first one is an inaccuracy of the efficiency determination within the method implemented for this procedure (see section 2.4), and is equal to 4%. It was calculated from the MC data by comparing the photon  $p_T$  distribution taken at the output of the event generator to the analogous distribution of reconstructed photons corrected for efficiency, the former being taken with the same cuts as the latter. The second component of the error above is related to the choice of the variables used to construct the efficiency tables. For example, the photon opening angle to the closest track can be used instead of the photon polar angle to the parent jet,  $\theta_\gamma$ . Another choice of an efficiency table variable could be the momentum of the closest track, or the jet charged multiplicity  $N_{ch}$  (note, all these variables make the efficiency sensitive to the track density near the jet axis). These possibilities were tried and indicate the uncertainty of this type in the efficiency finding to be about 5%.

In a similar way the appropriate systematic errors due to corrections for efficiency in individual bins of the photon  $p_T$  distribution were found.

## 4 Calculation of the inner bremsstrahlung

The principal sources of direct soft photons from the reaction (1) are expected to be bremsstrahlung from colliding  $e^+e^-$  (initial state radiation) and inner bremsstrahlung from final hadronic states. For soft photons both source rates can be calculated at once using either of two universal formulae:

- i) the formula, derivable from the Low paper [2] (see also [16,62]), explicitly displayed for the first time in [4] and then used by others [5–8,11]:

$$\frac{dN_\gamma}{d^3\vec{k}} = \frac{\alpha}{(2\pi)^2} \frac{1}{E_\gamma} \int d^3\vec{p}_1 \dots d^3\vec{p}_N \sum_{i,j} \eta_i \eta_j \frac{-(P_i P_j)}{(P_i K)(P_j K)} \frac{dN_{hadrons}}{d^3\vec{p}_1 \dots d^3\vec{p}_N} \quad (2)$$

where  $K$  and  $\vec{k}$  denote photon four- and three-momenta,  $P$  are four-momenta of beam  $e^+, e^-$  and of the  $N$  charged outgoing hadrons, and  $\vec{p}$  are three-momenta of the latter;  $\eta = 1$  for the beam electron and for positive outgoing hadrons,  $\eta = -1$  for the beam positron and negative outgoing hadrons, and the sum is extended over all the  $N + 2$  charged particles involved; the last factor in the integrand is a differential hadron production rate;

- ii) the Haissinski formula [63,64], which was tested to be more stable with respect to lost (undetected) particles and was used in [7,8,11]. It has the same form as (2) with the scalar products of four-vectors  $-(P_i P_j)$  being replaced by  $(\vec{p}_{i\perp} \cdot \vec{p}_{j\perp})$ , where  $\vec{p}_{i\perp} = \vec{p}_i - (\vec{n} \cdot \vec{p}_i) \cdot \vec{n}$  and  $\vec{n}$  is the photon unit vector.

It is known (see [8,11]), that the two formulae give results in complete agreement when used with MC generated particles unaffected by detector response, i.e. when all charged particles of an event enter into the formulae, with their precise momenta. We have tested the validity of this feature for our case in the following way. For every *reconstructed* jet the parameters of the *generated* charged particles lying in the forward hemisphere of the jet (including the corresponding beam particle) were collected and bremsstrahlung distributions for them were calculated, with the polar angle of the bremsstrahlung photon to the reconstructed jet direction being an angular variable. Note that this method, i.e. usage of *generated* particle momenta while projecting the produced photon onto the *reconstructed* jet direction, is both a) precise and b) automatically accounts for the angular resolution of the jet direction. Both formulae gave the same predictions, and these results were used in our estimates for the expected bremsstrahlung rates. Integrated over our kinematic range, the total bremsstrahlung rate was obtained to be  $17.1 \times 10^{-3} \gamma/\text{jet}$ ; after convolution with the detection efficiency, it drops to the value of  $0.340 \times 10^{-3} \gamma/\text{jet}$ . Note that the contribution of the ISR to these rates is small, being at the level of about 1.5% of them. The smallness is easy to explain: although the ISR from electron/positron beams is much more intense than the ISR from hadron beams in experiments [5–8,11], where it contributed a significant amount to the detected photon rate, all the extra photons in this experiment are emitted at very small polar angles with respect to the beam direction, with the angular distribution peaking at  $\Theta_\gamma = \sqrt{3}/\Gamma$ , where  $\Gamma$  is a beam Lorentz factor ( $\Gamma = 0.89 \times 10^5$  at the  $Z^0$  peak), thus yielding few photons in the barrel region.

The yield of the final state radiation from quarks of  $Z^0$  disintegrations is similarly small. For its estimate the photon implementation in JETSET [54] was used. The  $Q_0$  scale introduced for the QED part of the shower was varied<sup>3</sup> down to its natural lower limit, the constituent quark mass, which is  $300 \text{ MeV}/c^2$ . The production rate of photons off quarks in our kinematic range was found to be at the level of 3% of the hadronic bremsstrahlung rate<sup>4</sup>. In what follows, neither this nor the ISR yields will be discussed further; they are reduced in the RD–MC difference and will be ignored.

It follows from [3] that the applicability of the formulae above to the soft bremsstrahlung calculation is restricted in our case ( $e^+e^-$  annihilation into hadronic jets

<sup>3</sup>Together with these variations the QCD  $Q_0$  scale was varied within the range of 0.3 to  $2.25 \text{ GeV}/c^2$ , showing a weak influence of this cutoff on the production rate of soft photons off quarks.

<sup>4</sup>The situation changes little when decreasing the QED  $Q_0$  cutoff down to the extreme limit for it, which is about  $4 \text{ MeV}/c^2$ , due to a weak (logarithmic) dependence of the quark bremsstrahlung rate on the  $Q_0$ .

at  $\sqrt{s} = M_Z$ ) to the photon kinematic domain  $p_T \ll m_\pi c$ , which is a stronger condition than the one mentioned in the introduction for hadronic reactions. However, it has been verified (see next paragraph) that the applicability holds even at that weaker condition, with an accuracy of about 10%. Nevertheless, the stronger condition is also typically satisfied in our case since the  $p_T$  distribution of calculated inner hadronic bremsstrahlung with photons projected onto the plane perpendicular to the initial quark direction (i.e. before the spread induced by the angular resolutions) was found to peak at 30 MeV/ $c$ .

To test the applicability of the formula above the predictions for the initial state radiation calculated with this formula were compared with those of the DYMU3 generator [53]. For  $0.2 < E_\gamma < 1$  GeV bremsstrahlung photons produced within 100 mrad angles to the *beam* direction ( $P_T$  to the *beam* below 100 MeV/ $c$ ) the results coincided within 4%. For the photons produced within 100 mrad angles to a *jet* direction (the average  $P_T$  to the *beam* is 400 MeV/ $c$ ) the difference reached 11%. Since the range of the photon  $p_T$  under study in this work is restricted to be within 80 MeV/ $c$ , the estimate for the systematic error in the bremsstrahlung calculations due to formula (2) appears to be below 4% of the calculated bremsstrahlung rate. This error, together with further contributions to the bremsstrahlung calculation uncertainty described below, is given in table 2.

The stability of these calculations was tested using different event generators (JETSET, ARIADNE and HERWIG) and different jet finders (LUCLUS, DURHAM, JADE) obtaining bremsstrahlung rates agreeing within 5% when changing the generator (with LUCLUS as jet finder) and 3% when changing the jet finder (with JETSET as an event generator), see table 2.

Finally, when dealing with the results uncorrected for the detection efficiency, the generated bremsstrahlung distributions have to be convoluted with the efficiency. This induces an additional systematic error of 9% to the bremsstrahlung predictions due to the uncertainty in the efficiency determination. This error has two components, similar to those discussed at the end of section 3.2. The first one is an inaccuracy of the efficiencies within a given determination procedure (section 2.4), and is equal to 7%. It was calculated from the MC data by comparing the photon  $p_T$  distribution, taken at the output of the event generator and convoluted with the detection efficiency, on the one hand, to the analogous distribution of reconstructed photons (i.e. at the output of the MC stream), on the other hand. The other component of the error above is related to the choice of efficiency table variables and is equal to 5% of the calculated bremsstrahlung rate.

## 5 Experimental results

### 5.1 Photon distributions. Signal extraction

The results obtained in this study are presented both uncorrected and corrected for the photon detection efficiency. However, the principal set of results is given *uncorrected* for the efficiency. This is motivated by the fact that applying efficiency corrections increases both the statistical and systematic errors of the results. The latter occurs due to an uncertainty in the efficiency determination. The former happens because the entries with the smallest efficiency, i.e. with the largest weights, dominate the distributions. For example, with the efficiency corrections applied, the softest photons enter the distributions with weight factors up to one order of magnitude higher than those for the photons of moderate energy. Since this article is aimed mainly at the demonstration of the existence of excess photons, its principal results have to be presented with the highest possible

statistical and systematic accuracy. Therefore, efficiency-corrected results will be given only when the absolute photon rates are discussed, namely in section 5.2.

Thus we start with the  $\theta_\gamma, p_T$  and  $p_T^2$  photon distributions uncorrected for efficiency. The RD and MC distributions are presented in fig. 3 divided by and subtracted from each other. The RD–MC distributions (the right column of panels in fig. 3) are given in units of  $10^{-3}\gamma/\text{jet}$ , and are accompanied by calculated bremsstrahlung rates. All the distributions shown demonstrate an excess of soft photons in the RD as compared to the MC, and this excess is apparently higher than the expected bremsstrahlung level<sup>5</sup>.

To quantify the excess the difference between the RD and MC was integrated in the  $p_T$  interval from 0 to 80 MeV/c ( $p_T^2 < 0.64 \times 10^{-2} \text{ (GeV/c)}^2$ ), and the value obtained was defined as a signal. The excess of the RD over the MC as a function of  $p_T^2$  was fitted by an exponential. The results obtained are:

- signal rate

$$R_{RD-MC} = (1.17 \pm 0.06 \pm 0.27) \times 10^{-3}\gamma/\text{jet} \quad (3)$$

while the expected level of the hadronic photon background in this range taken from the MC is

$$R_{MC} = (18.40 \pm 0.04 \pm 0.26) \times 10^{-3}\gamma/\text{jet}. \quad (4)$$

The calculated level of the inner hadronic bremsstrahlung in the same range is, according to section 4,

$$R_{brems} = (0.340 \pm 0.001 \pm 0.038) \times 10^{-3}\gamma/\text{jet}. \quad (5)$$

Evaluated in terms of the inner bremsstrahlung rate, the signal is  $3.4 \pm 0.2 \pm 0.8$ . The rates (3) and (5) together with the other ones, obtained under various conditions described below, are given in table 3.

- the slope of the excess  $p_T^2$  distribution (assuming  $dN_\gamma/dp_T^2 \sim \exp(-Bp_T^2)$  for the excess photons) is fitted to the value of  $B = (251 \pm 21) \text{ (GeV/c)}^{-2}$ , which is also a good estimation for the slope of the inner hadronic bremsstrahlung, but is an order of magnitude steeper than the typical slopes of  $p_T^2$  distributions of photons in hadronic  $Z^0$  decays.

As can be seen from (3) and (5), the relative strength of the signal observed (i.e. signal strength expressed in terms of the bremsstrahlung rate) is comparable to the amplitudes of the anomalous soft photon effects seen in the hadronic beam experiments [5–8,11].

In order to check the independence of the signal amplitude on the jet-finding algorithm the DURHAM and JADE algorithms were applied to form jets instead of LUCLUS. The results were found to agree within the statistical errors, i.e. they are stable against the change of the jet-finding algorithm, see table 3. The LUCLUS to the DURHAM general selection signal ratio was found to be  $1.10 \pm 0.07$  and the LUCLUS to the JADE ratio was  $1.09 \pm 0.07$ .

## 5.2 Data corrected for efficiency

The  $\theta_\gamma, p_T$  and  $p_T^2$  photon distributions for the data corrected for the efficiency are given in the same form as those for the uncorrected ones and are displayed in fig. 4.

<sup>5</sup>There is a systematic excess of the bremsstrahlung predictions over the data at the angles  $\theta_\gamma > 200$  mrad. It comes from our recalibration procedure which assumed that no physical excess of photons exists at these angles. This assumption, invalid in principle since there exists a certain hadronic bremsstrahlung radiation at wide angles, induces a small systematic bias to the whole angular range due to an overcorrection and consequently lowers the observed photon excess rate. However, for the sake of clarity of the presentation we neglect this bias. Left neglected, it decreases the signal by an insignificant amount, while its accurate treatment would require including the bremsstrahlung calculation at wide angles into the procedure of the recalibration which we preferred to avoid here.

The integral signal rate (the RD to MC rate difference integrated over the  $p_T$  range from 0 to 80 MeV/ $c$ ) is  $(69.1 \pm 4.5 \pm 15.7) \times 10^{-3} \gamma/\text{jet}$  and is given in the last line of table 3. It is about 7% of the total jet rate, i.e. the absolute strength of the signal (the probability to have an excess photon per jet) is also similar to that found in the hadronic beam experiments<sup>6</sup>. The corresponding inner hadronic bremsstrahlung rate is  $(17.10 \pm 0.01 \pm 1.21) \times 10^{-3} \gamma/\text{jet}$ .

The differential signal rates ( $dN_\gamma/dp_T$  per 1000 jets) corrected for efficiency are presented in 10  $p_T$  bins in table 4, together with the corresponding predictions for the inner hadronic bremsstrahlung.

### 5.3 Zero signal experiment

In order to verify the analysis procedure it was applied to the photon kinematic domain where the anomalous soft photon excess was highly improbable (the zero experiment). Such a domain was defined as follows.

Instead of defining the photon kinematic variables with respect to the parent jet direction, the direction opposite to that of the most distant jet was chosen, while the acollinearity between this and the parent jet was required to be greater than 200 mrad. Thus, the procedure separates photons within the jets having an acollinear opposite jet and projects them onto the plane perpendicular to the direction of the latter. All other elements of the analysis were kept untouched, including the calculation of the bremsstrahlung predictions.

The photon distributions obtained with this procedure are shown in fig. 5 for the RD, for the MC, and for their difference. The latter distributions agree well with the bremsstrahlung predictions, though due to the relatively high statistical errors they are also compatible with zero in the range of  $p_T < 80$  MeV/ $c$ . The corresponding photon rates are given in table 3.

The results of the zero experiment have two different applications. First, they show that no anomalous photons are produced at the very beginning of the fragmentation process, before the first hard gluon emission. Had the photon radiation been produced at this stage (when two initial quarks are still highly collinear) the signal would be observed when relating the photon with the “antipode” of its parent jet, because the antipode jet would memorize the initial direction of the parent quark (which emits the photon in this scenario), unless a hard gluon emission deviates the antipode quark also.

The other use of the zero experiment is a confirmation of a good suppression of definite systematic effects, relevant also to our kinematic region and capable of producing a spurious excess. These effects are mainly of hardware systematics: an underestimation of material amount in front of the TPC in the MC code; a global difference in the reconstruction of the converted photons in the RD and MC; an improper treatment of background hits (noise, cosmics, etc.) in the RD by the pattern recognition program.

A quantitative estimation of possible biases induced by these effects has been given in section 3.1. Additional tests for these and other systematic effects are described in the following section.

---

<sup>6</sup>Here a correspondence of the photon production in a jet (this study) to its production in a minimum bias interaction event of the hadronic beam experiments is assumed.

## 6 Study of systematic biases capable of imitating the observed excess

### 6.1 Test for external bremsstrahlung

The most straightforward background capable of imitating the anomalous photon signal is the so called external bremsstrahlung, which is the bremsstrahlung from electrons (positrons) produced either in (semi)leptonic decays of hadrons or by internal or external conversion of photons from hadronic decays, when these electrons pass through the experimental setup. It also tends to peak at small  $p_T^2$ , and if it is underestimated by the MC, this could lead to an apparent excess of soft photons in the RD events. The rejection of jets containing at least one electron applied throughout this analysis (see section 2.5) was implemented in order to suppress this effect. However, electrons within the jets which escaped identification could be, in principle, responsible for the excess observed.

To check this hypothesis, the level of electron admixture in jets was varied from its natural ratio (dropping the rejection of jets containing identified electrons) to a 5 times smaller one, by applying a loose tag for the electron identification<sup>7</sup>. Thus, if an essential part of the signal comes from the electron bremsstrahlung, the signal rate should increase by several times when passing from the maximal rejection case (with loose electron tag) to the case with no rejection at all.

In fact, no enhancement of the signal rate was found when dropping the rejection of jets containing identified electrons (see table 3, lines 5,6), while the RD and MC rates both changed, by factors of  $1.0944 \pm 0.0055$  and  $1.0940 \pm 0.0038$ , respectively (the quoted numbers and their statistical errors are obtained with photons in the  $p_T < 80$  MeV/ $c$  range). Furthermore, the maximal electron rejection (with the loose tag, table 3, lines 7,8) does not decrease the signal, which should occur in the case of a contribution to the latter due to the external  $e^+e^-$  bremsstrahlung (the RD and MC rates decreased by factors of  $0.9386 \pm 0.0049$  and  $0.9400 \pm 0.0034$ , respectively).

Thus the hypothesis of an extra amount of the external bremsstrahlung from electrons inside the jets in the real data as a source of the excess appears to be excluded.

### 6.2 Changing MC generator

In order to check that the observed excess is not an artefact originating from a particular feature of the implemented MC generator (JETSET), the photon spectra produced with it were compared to those from ARIADNE. They are plotted in fig. 6. As can be seen from this figure, there is a rather weak prevalence of JETSET over ARIADNE at  $p_T$  below 80 MeV/ $c$ . This means that with ARIADNE as an event generator the excess of photons would be slightly increased. In amplitude, the observed difference is  $0.18 \times 10^{-3} \gamma/\text{jet}$ . Being expressed in the units of the signal strength, it is less than 15% in the photon  $p_T$  range below 80 MeV/ $c$ . This value is used as an estimate for the systematic error due to the event generator (section 3.2).

The comparison of JETSET with HERWIG shows a similar feature, with HERWIG data tending to decrease further the soft photon rate as compared to ARIADNE. Thus JETSET appears to be the generator giving the maximal soft photon yield among the tested event generators.

<sup>7</sup>The electron identification in DELPHI has different levels of electron tagging. Normally we used the standard tag, which provides electron identification with efficiency 55% for electrons having momenta above 2 GeV/ $c$  [46]. The loose tag has a higher electron identification efficiency, approaching 80%.



### 6.3 Secondary photons

When a high energy photon generates an  $e^+e^-$  pair in the material in front of the TPC the pair particles may radiate bremsstrahlung photons, which can enter our kinematic region. In most cases such photons have a small opening angle relative to the parent photon, which leads to a small-angle enhancement in the distribution of the two-photon opening angles. Such enhancements, at angles below 30 mrad, were seen in both the RD and MC distributions of the angles between two converted photons, but they cancelled in the RD/MC and RD–MC distributions. It follows from this that the given process is well reproduced in the MC stream and cannot be a source of the observed excess.

### 6.4 Comment on the pattern recognition bias

An important stage of the reconstruction of the converted photons is the reconstruction of their constituent  $e^+$  and  $e^-$  tracks from hits left by them in the TPC. A possible different treatment of the hits in the MC and RD by the pattern recognition would induce a systematic bias to the photon reconstruction efficiency. This difference may come from numerous sources. Two of them are listed below:

- in the case of the real data the TPC can be loaded by external tracks, noise, cosmics, etc., which is difficult to reproduce in the MC stream, thus resulting in different TPC patterns being fed into the reconstruction program of the RD and MC;
- a difference in the production of true hits from the  $e^+$  and  $e^-$  tracks of the photon conversion in the RD and the MC data may be induced by an improper setting of the TPC efficiency in the MC stream (e.g. simply due to TPC ageing), and may depend on the position of the photon conversion,  $e^+e^-$  track lengths (which vary with the photon energy) and even on the jet charged multiplicity, which produces a varying environment around the  $e^+e^-$  track hits.

This difference is expected to be reduced to a great extent by the recalibration procedure described in section 3.1. The only possible pattern recognition distinction between the RD and MC whose compensation is not ensured by this procedure can take place within the range of photon polar angles to the parent jet  $\theta_\gamma \leq 200$  mrad, since the wide angle photons ( $\theta_\gamma > 200$  mrad) were used for the recalibration. In this region the environment around the  $e^+e^-$  track hits may be affected by charged particles of the jet. In such a case the difference in the pattern recognition results should depend on the jet charged multiplicity. In order to test this possibility the RD to MC ratio was studied in several bands of the jet charged multiplicity, in three angular ranges:  $\theta_\gamma < 100$  mrad,  $100 \leq \theta_\gamma < 200$  mrad, and  $200 \leq \theta_\gamma < 400$  mrad. The ratios obtained for the different  $N_{ch}$  bands are in mutual agreement (within individual angular ranges) and agree well with the analogous global ratios of the RD to MC (table 5). This means that the pattern recognition results appear to be the same for the RD and MC within the full angular range under consideration.

### 6.5 Test with charged particles

The analysis of photon distributions described in sect. 5.1 was applied to artificial photons produced from charged pions. The aim of this test was to check that the hadronization procedure of the MC event generator in the soft kinematic region has no big systematic bias as compared to the analogous process in the real data. Being directly implemented for charged particles (which are charged pions mainly), it has a

straightforward relation to the  $\pi^0$  production also due to the almost precise SU(2) symmetry of the strong interactions<sup>8</sup> (earlier the idea of similar tests has been implemented in [4,5]). Thus, the method was to take three-momenta of charged particles in the real and MC data as a starting point to represent  $\pi^0$  distributions, to decay these “ $\pi^0$ ’s” into two photons, to convolute the resulting photon momenta with the photon detection efficiency and feed them into the analysis code.

The resulting distributions are shown in fig. 7. They are similar to the genuine photon spectra (cf. fig. 6), however the main result of this test is an excellent agreement between the RD and MC samples. The “signal” strength calculated in the same way as that for true photons is  $(0.102 \pm 0.014) \times 10^{-3} \gamma/jet$ , i.e. at the level of 9% of the photon signal (3). Therefore the hadronization mechanism of the applied MC code is concluded to work well as far as concerns the charged pion production. Being related via SU(2) symmetry with the production of neutral pions, it is expected to reproduce it sufficiently well too. The direct comparison of  $\pi^0$  production in the RD and MC is done in the next section.

## 6.6 $\pi^0$ tests

A general and powerful check of the adequacy of the MC data can be done via a comparison of the MC and RD  $\gamma\gamma$  mass spectra, by comparing the  $\pi^0$  signals detected in each data set. Note that the applicability of the results obtained with the  $\pi^0$  tests holds for almost the whole soft photon sample under study since the photon production in the data is dominated by  $\pi^0$  decays, which yield (according to the MC) almost 92% of photons in our kinematic range.

The production of  $\pi^0$ ’s in the DELPHI data of  $Z^0$  hadronic decays was studied in [47] including the  $\pi^0$ ’s arising from two converted photons. The experimental result for such  $\pi^0$ ’s shows a tendency for an overestimation of  $\pi^0$  production by JETSET 7.3 at low  $\pi^0$  momenta ( $< 1$  GeV/ $c$ ). However the results of that work cannot be used directly to estimate the systematic errors of the photon background rate in our kinematic range. Therefore a special analysis of  $\pi^0$  production was done in this work to get such an estimation from  $\pi^0$  signals extracted from the  $\gamma\gamma$  mass distributions of converted photons.

The photons (at least two converted photons per jet were required) were subdivided into two energy bands: one band of low energy (LE) 0.2-1 GeV, and one band of higher energy (HE) 1-10 GeV. Each HE photon was combined either with a LE photon of a given jet or with a HE photon. Both photons in the combination were weighted by the recalibration corrections. The  $\gamma\gamma$  mass distributions obtained are shown in fig. 8 for both, the MC and the RD. It can be seen from these distributions that there are distortions of the lower-mass parts of the  $\pi^0$  peaks. They are induced by the external bremsstrahlung radiation from at least one of the  $e^+e^-$  arms of a converted photon of the  $\pi^0$ . Therefore the spectra were fitted by two Gaussians superimposed over a smooth background, the second Gaussian being introduced to describe the distortions. The fit results have shown a small difference in the MC and RD widths of the first Gaussian,  $(4.0 \pm 0.1)$  MeV/ $c^2$  versus  $(4.4 \pm 0.1)$  MeV/ $c^2$ , respectively, for LE $\times$ HE combinations, and  $(4.8 \pm 0.1)$  MeV/ $c^2$  versus  $(5.6 \pm 0.1)$  MeV/ $c^2$  for HE $\times$ HE combinations. The  $\pi^0$  peak position was stable at 135 MeV/ $c^2$ , as well as the 2nd Gaussian parameters, the widths of the latter being 13 and 15 MeV/ $c^2$  for the LE $\times$ HE and HE $\times$ HE combinations, respectively. The ratio of the integrals under the two Gaussians (with the background subtracted) was found to

<sup>8</sup>There are processes which break the SU(2) symmetry (e.g. decays of  $\eta, \eta'$ ), but their contribution to the soft photon rate is small, see sect. 6.7.

be about two in both cases. The sum of the integrals under the Gaussians represents the number of  $\pi^0$ 's in an appropriate  $\gamma\gamma$  mass distribution. They are given <sup>9</sup> in table 6.

From the HE $\times$ HE results the HE photon RD to MC ratio was found to be  $1.020 \pm 0.007$ , i.e. the recalibration procedure succeeded in reducing the RD and MC difference to the level of 2% for these photons. For the LE photons the effect of the recalibration seems to be slightly better, the RD to MC ratio deduced from the LE $\times$ HE results is  $0.986 \pm 0.023$  taking into account the factor 1.020 of the HE photon ratio obtained above. This agrees well with the recalibration results for the difference residuals discussed in section 3.1 and illustrated by fig. 2.

Thus the upper limit for the systematic bias of soft photon RD to MC ratio which can be obtained from the  $\pi^0$  test with converted photons is 1.024 at the 95% C.L.

In order to get an independent check of this result the whole procedure described above was repeated replacing the HE converted photon with a calorimetric (HPC) photon in the same energy band and within a  $\Theta_\gamma$  range of  $50^\circ - 130^\circ$ . The HPC photons were combined with LE and HE converted photons being weighted by the second type of the recalibration procedure, i.e. with the energy binning. In spite of a worse mass resolution (by a factor of 4), the statistical gain due to combination of converted photons with those from the HPC was expected to give a statistical accuracy of the fit results comparable to those obtained with two converted photon analysis. Since the HPC photons may have their own systematic bias, the HPC $\times$ HPC combinations were also involved in the analysis.

The  $\gamma\gamma$  mass distributions for these photon combinations are displayed in fig. 9. No distortion effects are visible in the distributions due to the worse mass resolution and due to a smaller yield of the converted photons to the spectra of a) to d) (by a factor of two). The distributions were therefore fitted with a single Gaussian superimposed over a smooth background. The results of the fit for the numbers of  $\pi^0$ 's are given in table 7.

It follows from these results that the converted HE photon RD to MC ratio is  $1.014 \pm 0.013$  if one takes into account the proper HPC RD to MC bias  $1.011 \pm 0.004$  obtained from the HPC $\times$ HPC signals. This ratio agrees well with the double converted photon analysis value  $1.020 \pm 0.007$ . The converted LE photon RD to MC ratio is then  $0.985 \pm 0.028$  and the upper limit for the systematic bias of the converted soft photon RD to MC ratio obtained from this test is 1.031 at the 95% C.L.

Thus, the two analyses agree and suggest that there is no excess of LE photons from  $\pi^0$  decays in our kinematic range. A combined upper limit for such an excess derived from both analyses is 1.015 at the 95% C.L. This means that the observed soft photon signal is 4 times greater than the 95% C.L. upper limit resulting from the identity of the  $\pi^0$  production rates in the RD and MC.

These results, in favour of the absence of any non-negligible systematic bias in the current analysis obtained with the  $\pi^0$  tests, are of high importance due to the fact that the photon production in hadronic  $Z^0$  events is dominated by  $\pi^0$  decays, as mentioned above. Small admixtures from radiative decays of  $B^*$  mesons,  $\eta$ 's,  $\Sigma^0$  baryons and other unstable particles to the overall soft photon production rate are not significant and have been verified not to change the above conclusion on the systematic bias estimations, as discussed in the next section.

## 6.7 Soft photons from unstable hadrons other than $\pi^0$ 's

The strongest sources of soft photons from unstable hadrons other than  $\pi^0$ 's in hadronic  $Z^0$  decays are  $B^*$  mesons which have dominant radiative branching ratios and low decay

<sup>9</sup>We do not give the individual Gaussian yields since they interfere strongly due to pile-up of the Gaussians, while their sum is close to being fit invariant.

momenta. According to the MC, neutral and charged  $B^*$  mesons yield 3.3% and 2.7% of the total soft photon rate in our kinematic range, respectively.

In order to check that there is no bias in the DELPHI MC simulation of soft photons from the  $B^*$  meson decays, the  $B$  meson admixture in the data under study was varied using the DELPHI B tag [65]. It was found that the signal is stable (within the quoted errors) when varying the  $B^*$  photon yield in our kinematic range by a factor of 40, from 0.3% with depleted  $B^*$  production (the anti-B tag applied) to 12% with enriched  $B^*$  production (the B tag applied), the corresponding results are presented by lines 9 and 10 in table 3, respectively.

The reason for this stability is easy to understand. Since the observed soft photon signal is of similar strength to the whole relative yield of  $B^*$  mesons (both are at about 6% of the total soft photon rate), the DELPHI MC would have to be wrong in the prediction of the  $B^*$  production rate by about 100% to allow the signal to come from these mesons. This is completely excluded by the good agreement between the MC and real data for the  $B^*$  signal amplitude and its characteristics, studied in [60], from which the discrepancy between the two data sets is deduced to be below 4%.

This fact was used for an independent proof of the statement that an improper simulation of soft photons from the  $B^*$  meson decays cannot be responsible for the signal observed. Making use of the  $B^*$  photon yield in our kinematic range (6%, see above) and the experimental agreement of the  $B^*$  production rate with the simulation, the systematic uncertainty in the total soft photon rate due to  $B^*$  photons is established to be below 0.3%. In absolute value, using the total soft photon production rate (4), it is less than  $0.05 \times 10^{-3} \gamma/\text{jet}$ . This uncertainty is quoted in table 1.

Similar considerations are applicable to other unstable particles. Therefore the yields of  $\eta$ 's,  $\Sigma^0$  baryons and other radiatively decaying hadrons ( $\omega^0$ ,  $D^*$  mesons, etc.) to our photon kinematic range were estimated studying the MC data and published results on their total production rates [66–68].

It was found from the MC data that the yield of  $\eta$  mesons to our photon kinematic range is  $(1.03 \pm 0.01)\%$ , the quoted error being statistical. The systematic error of this estimate can be obtained by comparing the MC and experimental  $\eta$  meson total production rates [66]. They agree within 10% [69] which leads to an error in the overall soft photon production rate induced by the  $\eta$  decays of less than 0.1%, or below  $0.02 \times 10^{-3} \gamma/\text{jet}$ . This uncertainty, though relatively small, is included into the software systematic error list quoted in table 1.

The photon yields from  $\Sigma^0$  baryons,  $D^*$  and other unstable hadrons to our kinematic range are even smaller due to their lower radiative branching ratios and/or higher decay momenta, thus the systematic uncertainties due to them can be neglected.

Finally, the hypothetical situation when the excess photons originate from unstable hadrons which are among  $Z^0$  decay products, but are not incorporated (or not incorporated properly) in the implemented MC event generators, was considered. The method was to calculate the photon  $p_T^2$  spectrum from radiative decays of an *a priori* unknown unstable (excited) hadron, the excitation energy being varied in a wide range (from 35 to 500 MeV; the mass of the hadron was varied also, from 1 to 5 GeV/ $c^2$ , and was found to affect the results very slightly), and to compare the shape of the obtained spectrum with that of the observed excess. In order to account for a diversity of possible kinematic characteristics of the assumed hadron (its energy spectrum and angular distribution relative to a jet) various energy and angular distributions of a large number of unstable hadrons were obtained from the DELPHI MC data and used as templates when generating the

results. Given all the needed input parameters, the photon  $p_T^2$  spectra were calculated using two-body decay phase space formulae.

It was found that only very low excitation energies (below 40 MeV) combined with a narrow angular distribution of the excited hadron are able to produce the exponentially decreasing  $p_T^2$  spectra similar to that of the observed excess (section 5.1). However, no state with such an excitation energy is present in the PDG tables [70]. The nearest candidate for such a state is the  $B^*$  (with the excitation energy of 46 MeV), but this state is well incorporated into the DELPHI MC and was directly tested varying the  $B^*$  yield as described above.

From these results the conclusion is drawn that no known hadron decaying radiatively can be a source of a viable systematic effect to the observed signal.

## 7 Conclusions

This analysis shows a significant excess of soft photons close to jet axes in the hadronic decays of the  $Z^0$  collected in the DELPHI experiment at LEP1, as compared to the Parton Shower MC predictions. The photon kinematic range is defined as follows:  $0.2 < E_\gamma < 1$  GeV,  $p_T < 80$  MeV/ $c$ , the  $p_T$  being the photon transverse momentum with respect to the parent jet direction. The net excess is measured to be  $(1.17 \pm 0.06 \pm 0.27) \times 10^{-3} \gamma/jet$  for the data uncorrected for the photon detection efficiency. This value has to be compared to the calculated level of the inner hadronic bremsstrahlung which was expected to be the dominant source of direct soft photons in this kinematic region (but which was not implemented in the standard MC codes used) and is obtained to be  $(0.340 \pm 0.001 \pm 0.038) \times 10^{-3} \gamma/jet$ . Expressed in terms of the bremsstrahlung rate, the observed signal is  $3.4 \pm 0.2 \pm 0.8$ .

The various systematic biases capable of producing the excess photons were carefully studied, leading to the conclusion that the origin of the excess cannot be attributed to trivial reasons such as an underestimation of the external bremsstrahlung in the MC events, improper simulation of the soft photon spectra by an event generator or different treatment of the real and MC data by the pattern recognition code. An important point is the good agreement between the MC and real data concerning the production and detection of  $\pi^0$ 's when one of the photons of the  $\pi^0$  decay is soft.

Analogous conclusions can be drawn for the data corrected for the photon detection efficiency: the observed signal rate is found to be  $(69.1 \pm 4.5 \pm 15.7) \times 10^{-3} \gamma/jet$ , while the inner bremsstrahlung rate is expected to be  $(17.10 \pm 0.01 \pm 1.21) \times 10^{-3} \gamma/jet$ . Their ratio is then  $4.0 \pm 0.3 \pm 1.0$ .

The signal amplitudes obtained are close to the anomalous soft photon effects seen earlier in hadronic reactions at high energy and reported in [5–8,11].

## Acknowledgements

We are grateful to Profs. K. Boreskov, A. Kaidalov, O. Kancheli, L. Okun, Yu. Simonov, T. Sjöstrand and P. Sonderegger for useful discussions, and to Dr. B. French for detailed considerations of several aspects of this work.

We are greatly indebted to our technical collaborators, to the members of the CERN-SL Division for the excellent performance of the LEP collider, and to the funding agencies for their support in building and operating the DELPHI detector.

We acknowledge in particular the support of

Austrian Federal Ministry of Education, Science and Culture, GZ 616.364/2-III/2a,98,  
FNRS-FWO, Flandres Institute to encourage scientific and technological research in the  
industry (IWT), Belgium,  
FINEP, CNPq, CAPES, FUJB and FAPERJ, Brazil,  
Czech Ministry of Industry and Trade, GA CR 202/99/1362,  
Commission of the European Communities (DG XII),  
Direction des Sciences de la Matière, CEA, France,  
Bundesministerium für Bildung, Wissenschaft, Forschung und Technologie, Germany,  
General Secretariat for Research and Technology, Greece,  
National Science Foundation (NSF) and Foundation for Research on Matter (FOM),  
The Netherlands,  
Norwegian Research Council,  
State Committee for Scientific Research, Poland, SPUB-M/CERN/P03/DZ296/2000,  
SPUB-M/CERN/P03/DZ297/2000, 2PO3B 104 19 and 2PO3B 69 23(2002-2004),  
FCT - Fundação para a Ciência e Tecnologia, Portugal,  
Vedecka grantova agentura MS SR, Slovakia, Nr. 95/5195/134,  
Ministry of Science and Technology of the Republic of Slovenia,  
CICYT, Spain, AEN99-0950 and AEN99-0761,  
The Swedish Research Council,  
Particle Physics and Astronomy Research Council, UK,  
Department of Energy, USA, DE-FC02-01ER41155,  
EEC RTN contract HPRN-CT-00292-2002.

## References

- [1] L.D. Landau, I.Ya. Pomeranchuk, Dokl. Akad. Nauk SSSR **92**, 535, 735 (1953) (Papers No. 75 and 76 in the English edition of L.D. Landau collected works)
- [2] F. Low, Phys. Rev. **110**, 974 (1958)
- [3] V.N. Gribov, Sov. J. Nucl. Phys. **5**, 280 (1967)
- [4] A.T. Goshaw et al., Phys. Rev. Lett. **43**, 1065 (1979)
- [5] P.V. Chliapnikov et al., Phys. Lett. B **141**, 276 (1984)
- [6] F. Botterweck et al., Z. Phys. C **51**, 541 (1991)
- [7] S. Banerjee et al., Phys. Lett. B **305**, 182 (1993)
- [8] A. Belogianni et al., Phys. Lett. B **408**, 487 (1997)  
A. Belogianni et al., Phys. Lett. B **548**, 122 (2002)
- [9] M.L. Tincknell et al., Phys. Rev. C **54**, 1918 (1996)
- [10] J. Antos et al., Z. Phys. C **59**, 547 (1993)
- [11] A. Belogianni et al., Phys. Lett. B **548**, 129 (2002)
- [12] A. Bogolyubski et al., Sov. J. Nucl. Phys. **49**, 454 (1989)
- [13] L. Van Hove, Ann. of Phys. **192**, 66 (1989)
- [14] S. Barshay, Phys. Lett. B **227**, 279 (1989); Erratum-ibid. **245**, 687 (1990)
- [15] E.V. Shuryak, Phys. Lett. B **231**, 175 (1990)
- [16] V. Balek, N. Pišútová and J. Pišút, Acta Phys. Pol. B **21**, 149 (1990)
- [17] P. Lichard, L. Van Hove, Phys. Lett. **B45**, 605 (1990)
- [18] V. Balek et al., Acta Phys. Slovaca **41**, 86 (1991)
- [19] V. Balek, N. Pišútová and J. Pišút, Acta Phys. Slovaca **41**, 158 (1991)
- [20] S.M. Darbinian, K.A. Ispirian, A.T. Margarian, Sov. J. Nucl. Phys. **54**, 364 (1991)
- [21] P. Lichard, J.A. Thompson, Phys. Rev. D **44**, 668 (1991)
- [22] P. Lichard, Phys. Rev. D **50**, 6824 (1994)
- [23] W. Czyż, W. Florkovski, Z. Phys. C **61**, 171 (1994)
- [24] S. Barshay, Particle World **3**, 180 (1994)
- [25] S. Barshay, P. Heiliger, Z. Phys. C **64**, 675 (1994)
- [26] S. Barshay, P. Heiliger, Z. Phys. C **66**, 459 (1995)
- [27] O. Nachtmann, in *Proceedings of 18th Johns Hopkins Workshop on Current Problems in Particle Theory, Florence, 1994*, (World Sci., Singapore, New Jersey, London, Hong Kong 1994), p. 143; hep-ph/9411345
- [28] G.W. Botz, P. Haberl, O. Nachtmann, Z. Phys. C **67**, 143 (1995)
- [29] O. Nachtmann, in *Proceedings of 35th International University School of Nuclear and Particle Physics: Perturbative and Nonperturbative Aspects of Quantum Field Theory, Schlading, 1996*, edited by H. Latal and W. Schweiger (Springer 1996), p. 49; hep-ph/9609365
- [30] E. Quack, P.A. Hennig, Phys. Rev. D **54**, 3125 (1996)
- [31] J. Pišút, N. Pišútová, B. Tomášik, Phys. Lett. B **368**, 179 (1996)
- [32] Z. Huang, X.N. Wang, Phys. Lett. B **383**, 457 (1996)
- [33] E.S. Kokoulina, *Gluon Dominance Model*, to appear in *Proceedings of 35th International Symposium on Multiparticle Dynamics (ISMD 05), Kromeriz, 2005*; hep-ph/0511111, hep-ph/051114  
P.F. Ermolov et al., *Study of Multiparticle Production by Gluon Dominance Model*, hep-ph/0503254
- [34] H.G. Dosh, Yu.A. Simonov, Phys. Lett. B **205**, 339 (1988)

- [35] OPAL Collaboration, M.Z. Akrawy et al., Phys. Lett. B **246**, 285 (1990)
- [36] OPAL Collaboration, P.D. Acton et al., Z. Phys C **54**, 193 (1992)  
OPAL Collaboration, R. Akers et al., Z. Phys. C **67**, 15 (1995)
- [37] OPAL Collaboration, G. Alexander et al., Phys. Lett. B **264**, 219 (1991)  
OPAL Collaboration, P.D. Acton et al., Z. Phys. C **58**, 405 (1993)
- [38] OPAL Collaboration, K.W. Bell et al., Nucl. Phys. (Proc. Suppl.) B **64**, 32 (1998)
- [39] L3 Collaboration, O. Adriani et al., Phys. Lett. B **262**, 155 (1991)  
L3 Collaboration, O. Adriani et al., Phys. Lett. B **292**, 472 (1992)  
L3 Collaboration, M. Acciarri et al., Phys. Lett. B **353**, 136 (1995)
- [40] L3 Collaboration, O. Adriani et al., Phys. Lett. B **301**, 136 (1993)
- [41] DELPHI Collaboration, P. Abreu et al., Z. Phys. C **53**, 555 (1992)
- [42] DELPHI Collaboration, P. Abreu et al., Z. Phys. C **69**, 1 (1995)
- [43] ALEPH Collaboration, D. Decamp et al., Phys. Lett. B **264**, 476 (1991)
- [44] ALEPH Collaboration, D. Buskulic et al., Z. Phys. C **57**, 17 (1993)
- [45] DELPHI Collaboration, P. Aarnio et al., Nucl. Instr. and Meth. A **303**, 233 (1991)
- [46] DELPHI Collaboration, P. Abreu et al., Nucl. Instr. and Meth. A **378**, 57 (1996)
- [47] DELPHI Collaboration, W. Adam et al., Z. Phys. C **69**, 561 (1996)
- [48] T. Sjöstrand, Comput. Phys. Commun. **39**, 347 (1986)  
T. Sjöstrand, M. Bengtsson, Comput. Phys. Commun. **43**, 367 (1987)  
T. Sjöstrand, *JETSET 7.3 Program and Manual*, CERN-TH/6488-92, 1992
- [49] H. Fürstenau, *Corrected Data Distribution and Monte Carlo Tuning*, DELPHI note 93-17 PHYS-264, 1993; H. Fürstenau, *Tests of QCD and Grand Unified Theories with the DELPHI Detector at LEP*, Ph.D. thesis 04/12/92, University of Karlsruhe, 1992; KA-IEKP 92-16, 1992
- [50] DELPHI Collaboration, P. Abreu et al., Z. Phys. C **73**, 11 (1996)
- [51] L. Lönnblad, Comput. Phys. Commun. **71**, 15 (1992)
- [52] G. Marchesini et al., Comput. Phys. Commun. **67**, 465 (1992)
- [53] J.E. Campagne, R. Zitoun, Z. Phys. C **43**, 469 (1989)  
J.E. Campagne et al. in: Z Physics at LEP1, G. Altarelli, R. Kleiss and C. Verzegnassi eds., CERN Yellow Report No.89-08, 1989, vol.3, 2.2.5, 3.2.5
- [54] T. Sjöstrand, in: Workshop on Photon Radiation from Quarks, S. Cartwright ed., CERN Yellow Report No.92-04, 1992, p.103
- [55] T. Sjöstrand, Comput. Phys. Commun. **28**, 227 (1983)  
T. Sjöstrand, Comput. Phys. Commun. **82**, 74 (1994)  
T. Sjöstrand, CERN-TH/7112-93, 1993
- [56] S. Catani, Yu.L. Dokshitzer, M. Olsson, G. Turnock, B.R. Webber, Phys. Lett. B **269**, 432 (1991)  
S. Bethke, Z. Kunszt, D.E. Sopper, W.J. Stirling, Nucl. Phys. B **370**, 310 (1992)
- [57] JADE Collaboration, W. Bartel et al., Z. Phys. C **33**, 23 (1986)  
JADE Collaboration, S. Bethke et al., Phys. Lett. B **213**, 235 (1988)
- [58] W.T. Eadie et al., *Statistical Methods in Experimental Physics* (North-Holland, Amsterdam, 1982) p. 90
- [59] S. Moretti, L. Lönnblad, T. Sjöstrand, JHEP 9808:0001 (1998); hep-ph/9804296
- [60] DELPHI Collaboration, P. Abreu et al., Z. Phys. C **68**, 353 (1995)



- [61] G. Gustavson, U. Peterson, Nucl. Phys. B **308**, 746 (1988)
- [62] T.H. Burnett, N.M. Kroll, Phys. Rev. Lett. **20**, 86 (1968)  
L.D. Landau, V.B. Berestetskii, E.M. Lifshitz, L.P. Pitaevskii, *Relativistic Quantum Theory, pt.1*, (Pergamon, Oxford 1971)  
J.D. Jackson, *Classical Electrodynamics*, 3rd edn. (John Wiley, New York, Chichester, Weinheim, Brisbane, Singapore, Toronto 1999)
- [63] J. Haissinski, *How to Compute in Practice the Energy Carried away by Soft Photons to all Orders in  $\alpha$* , LAL 87-11, 1987
- [64] M. Grabowski, U. Kerres, (SOPHIE/WA83) Internal Note 6.10.87 (Unpublished), 1987  
T.J. Brodbeck (for WA83 Collaboration), in *Proceedings of Cracow Workshop on Multiparticle Production, 1993*, edited by A. Bialas, K. Fialkowski, K. Zalewski and R.C. Hwa (World Sci., Singapore, New Jersey, London, Hong Kong 1993), p. 63
- [65] DELPHI Collaboration, J. Abdallah et al., Eur. Phys. J. C **32**, 185 (2004)
- [66] ALEPH Collaboration, D. Buskulic et al., Phys. Lett. B **292**, 210 (1992)  
L3 Collaboration, M. Acciari et al., Phys. Lett. B **328**, 223 (1994)  
OPAL Collaboration, K. Ackerstaff et al., Eur. Phys. J. C **5**, 411 (1998)
- [67] DELPHI Collaboration, W. Adam et al., Z. Phys. C **70**, 371 (1996)  
OPAL Collaboration, G. Alexander et al., Z. Phys. C **73**, 587 (1997)  
ALEPH Collaboration, R. Barate et al., Phys. Lett B **366**, 1 (1998)
- [68] DELPHI Collaboration, P. Abreu et al., Eur. Phys. J. C **12**, 209 (2000)
- [69] P.V. Chliapnikov, V.A. Uvarov, Phys. Lett. B **435**, 313 (1995)
- [70] S. Eidelman et al., Review of Particle Physics, Phys. Lett. B **592**, 1 (2004)

**Table 1.** Systematic uncertainties of the background of hadronic decay photons in the range of photon  $p_T < 80$  MeV/ $c$  for the data uncorrected for detection efficiency. The total systematic error is the quadratic sum of the individual errors.

Source	Value, $10^{-3}\gamma/\text{jet}$	Percentage of signal rate <sup>*)</sup>
Hardware systematics		
Material uncertainty and pattern recognition	0.16	14
Software systematics		
Event generator	0.20	17
Jet finder	0.07	6
$B^*$ mesons	0.05	4
$\eta$ mesons	0.02	2
Total	0.27	23

<sup>\*)</sup> The signal rate is defined in section 5.1.

**Table 2.** Systematic uncertainties of the inner hadronic bremsstrahlung calculations in the range of photon  $p_T < 80$  MeV/ $c$ . The total systematic error is the quadratic sum of the individual errors. The uncertainties, given in absolute photon rates (2nd column of the table) correspond to the case of the data uncorrected for detection efficiency.

Source	Value, $10^{-3}\gamma/\text{jet}$	Percentage of brems rate
Formula (2)	0.014	4
Event generator	0.017	5
Jet finder	0.010	3
Convolution with efficiency <sup>*)</sup>	0.029	9
Total	0.038	11

<sup>\*)</sup> The systematic error due to convolution with efficiency has to be taken into account when dealing with the results uncorrected for efficiency only.

**Table 3.** Signal amplitudes in units of  $10^{-3}\gamma$  per jet, obtained under various selection criteria. The jets satisfy all the selection cuts described in section 2.5 and additional cuts (if any), as indicated in this table. The jets were formed by the LUCLUS jet-finding code unless the DURHAM or JADE codes are referred to explicitly. The errors are statistical only. Information on the systematic errors of the experimental photon rates and the bremsstrahlung predictions is given in tables 1 and 2, respectively.

	Selection conditions	Signal	Brems
1	General selection	$1.170\pm 0.062$	$0.340\pm 0.001$
2	General selection, DURHAM	$1.060\pm 0.067$	$0.351\pm 0.001$
3	General selection, JADE	$1.070\pm 0.074$	$0.332\pm 0.001$
4	The zero experiment	$0.069\pm 0.048$	$0.0750\pm 0.0002$
5	No rejection of jets containing $e^+, e^-$	$1.170\pm 0.061$	$0.339\pm 0.001$
6	No rejection of jets containing $e^+, e^-$ , DURHAM	$1.050\pm 0.066$	$0.348\pm 0.001$
7	Strong rejection of jets with $e^+, e^-$	$1.150\pm 0.062$	$0.326\pm 0.001$
8	Strong rejection of jets with $e^+, e^-$ , DURHAM	$1.050\pm 0.067$	$0.336\pm 0.001$
9	General selection + anti-B tag	$1.240\pm 0.167$	$0.363\pm 0.002$
10	General selection + B tag	$1.390\pm 0.159$	$0.326\pm 0.002$
	General selection, signal corrected for efficiency	$69.1\pm 4.5$	$17.10\pm 0.01$

**Table 4.** Differential signal and inner hadronic bremsstrahlung rates as a function of the photon  $p_T$ , in units of  $10^{-3}\gamma/\text{jet}$  integrated over the  $p_T$  bin of 8 MeV/ $c$  width. The first errors are statistical, the second ones are systematic.

$p_T$ , MeV/ $c$	RD–MC corrected for efficiency	Inner hadronic bremsstrahlung
0 - 8	$0.64 \pm 0.38 \pm 0.14$	$0.685 \pm 0.001 \pm 0.048$
8 - 16	$2.66 \pm 0.84 \pm 0.63$	$1.584 \pm 0.002 \pm 0.112$
16 - 24	$6.48 \pm 1.18 \pm 1.46$	$1.928 \pm 0.002 \pm 0.136$
24 - 32	$8.31 \pm 1.40 \pm 1.83$	$2.007 \pm 0.002 \pm 0.142$
32 - 40	$11.01 \pm 1.55 \pm 2.46$	$1.984 \pm 0.002 \pm 0.140$
40 - 48	$8.88 \pm 1.69 \pm 2.03$	$1.926 \pm 0.001 \pm 0.136$
48 - 56	$9.70 \pm 1.66 \pm 2.25$	$1.850 \pm 0.001 \pm 0.131$
56 - 64	$6.61 \pm 1.62 \pm 1.52$	$1.776 \pm 0.001 \pm 0.126$
64 - 72	$7.30 \pm 1.60 \pm 1.67$	$1.704 \pm 0.001 \pm 0.121$
72 - 80	$7.58 \pm 1.61 \pm 1.76$	$1.635 \pm 0.001 \pm 0.116$

**Table 5.** RD to MC ratios in three ranges of  $\theta_\gamma$  as a function of the jet charged multiplicity  $N_{ch}$ .

$N_{ch}$ band	$\theta_\gamma < 100\text{mrad}$	$100\text{mrad} \leq \theta_\gamma < 200\text{mrad}$	$200\text{mrad} \leq \theta_\gamma < 400\text{mrad}$
$1 \leq N_{ch} \leq 3$	$1.060 \pm 0.013$	$1.046 \pm 0.010$	$0.980 \pm 0.009$
$3 < N_{ch} \leq 5$	$1.074 \pm 0.010$	$1.025 \pm 0.007$	$1.001 \pm 0.006$
$5 < N_{ch} \leq 7$	$1.049 \pm 0.009$	$1.044 \pm 0.007$	$0.973 \pm 0.006$
$N_{ch} > 7$	$1.067 \pm 0.007$	$1.028 \pm 0.006$	$1.005 \pm 0.005$
all $N_{ch}$	$1.064 \pm 0.005$	$1.033 \pm 0.004$	$0.994 \pm 0.003$

**Table 6.**  $\pi^0$  signal amplitudes (numbers of  $\pi^0$ 's in the  $\pi^0$  peaks) obtained with two combinations of converted photons and the upper limits for the RD/MC ratio of the converted LE photons extracted from the signals.

	$\text{LE}_{\text{conv}} \times \text{HE}_{\text{conv}}$	$\text{HE}_{\text{conv}} \times \text{HE}_{\text{conv}}$
RD	$9052 \pm 147$	$19529 \pm 206$
MC	$8999 \pm 133$	$18774 \pm 154$
RD/MC	$1.006 \pm 0.022$	$1.040 \pm 0.013$
Resulting RD/MC for the LE photons: $0.986 \pm 0.023$		
Upper limit for the converted LE photon RD/MC ratio (at 95% C.L.): 1.024		

**Table 7.**  $\pi^0$  signal amplitudes obtained with three combinations of converted and HPC photons and the upper limits for the RD/MC ratio of the converted LE photons extracted from the signals. The combined upper limit is a summary of both  $\pi^0$  analyses (see table 6).

	$\text{LE}_{\text{conv}} \times \text{HE}_{\text{HPC}}$	$\text{HE}_{\text{conv}} \times \text{HE}_{\text{HPC}}$	$\text{HE}_{\text{HPC}} \times \text{HE}_{\text{HPC}}$
RD	$38396 \pm 803$	$91262 \pm 905$	$1182370 \pm 5890$
MC	$38539 \pm 687$	$89065 \pm 690$	$1156220 \pm 4950$
RD/MC	$0.996 \pm 0.027$	$1.025 \pm 0.013$	$1.023 \pm 0.007$
Resulting RD/MC for the LE photons: $0.985 \pm 0.028$			
Upper limit for the converted LE photon RD/MC ratio (at 95% C.L.): 1.031			
<b>Combined upper limit for the converted LE photon RD/MC ratio: 1.015</b>			

# DELPHI

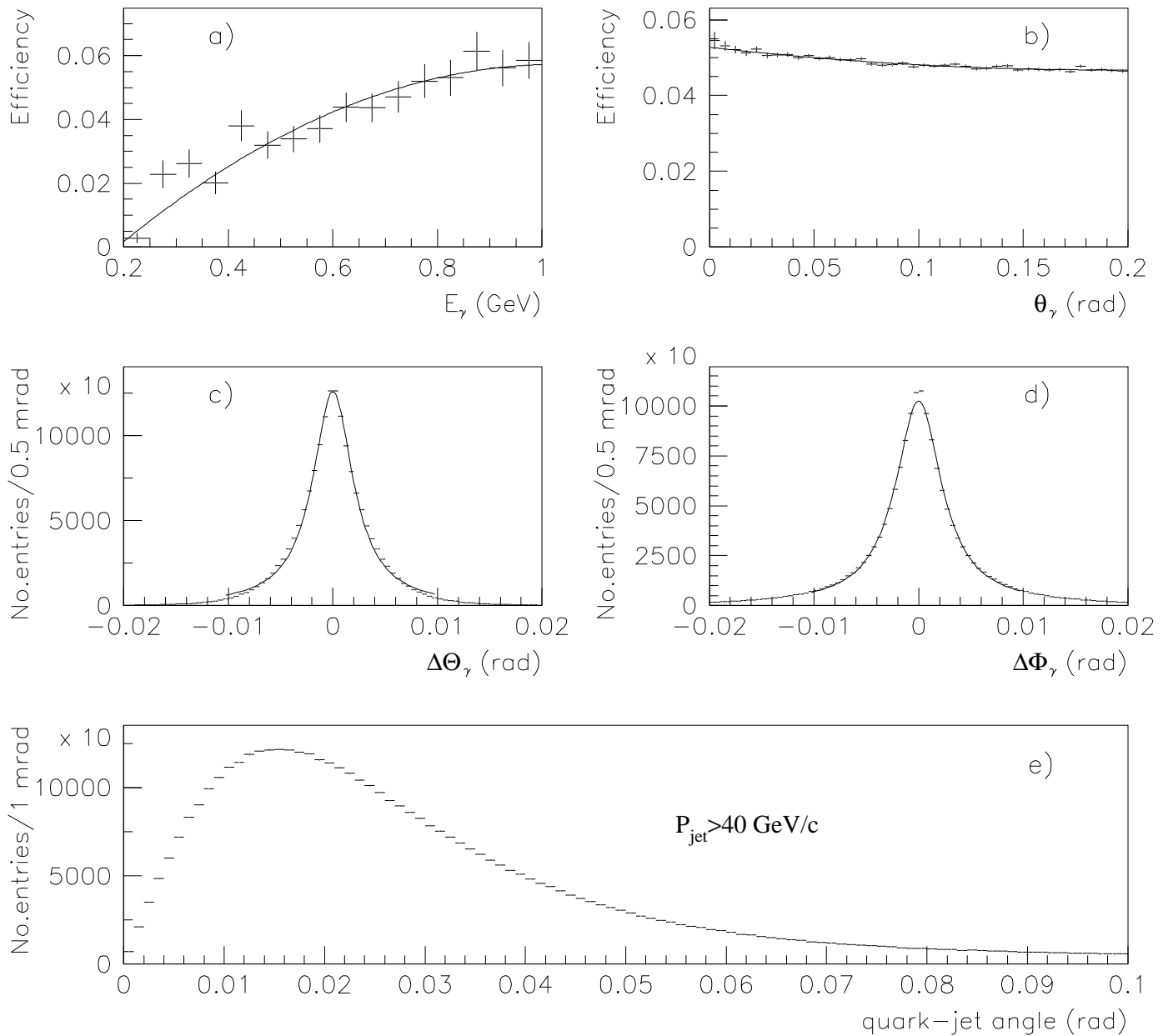


Figure 1: a) Photon detection efficiency as a function of the photon energy in the angular band of  $\theta_\gamma < 5$  mrad (the statistically poorest angular band) integrated over the 3rd efficiency table variable,  $\Theta_\gamma$ ; b) photon detection efficiency as a function of  $\theta_\gamma$  in the  $E_\gamma$  band from 0.9 to 1 GeV (the region of the highest efficiency) integrated over  $\Theta_\gamma$ ; c) difference between generated and reconstructed photon polar angles  $\Theta_\gamma$  in the photon energy range of  $0.2 < E_\gamma < 1$  GeV; d) the same for the azimuthal angles  $\Phi_\gamma$ ; e) deviation of the reconstructed jet axis from the initial quark direction for jet momenta  $> 40$  GeV/c. The curves in figs. 1a,b) are 2nd order polynomial fits used for the efficiency interpolation. The curves in figs. 1c,d) are the fits by Breit-Wigner form's (see text).

# DELPHI

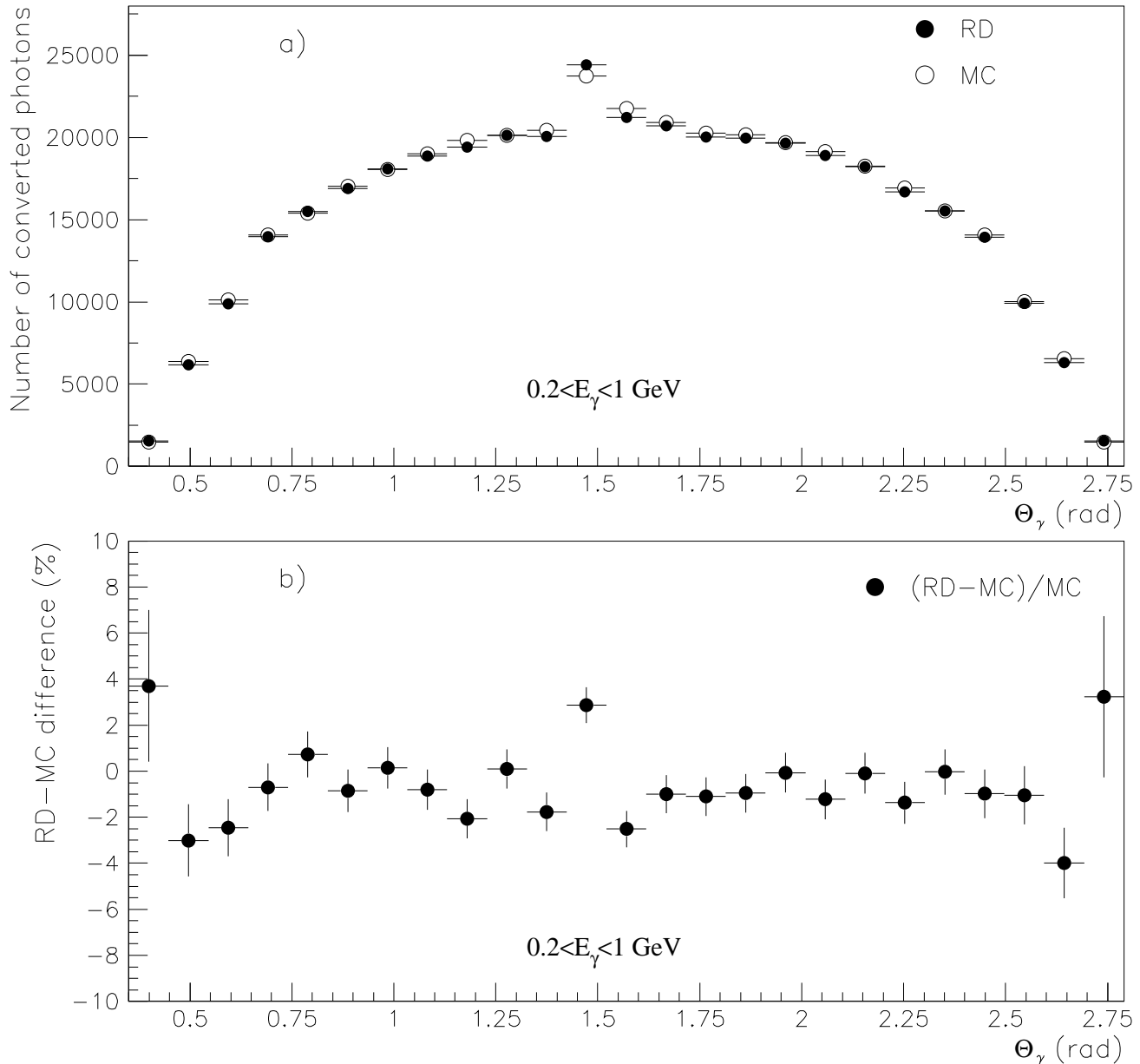


Figure 2: a) The RD and MC angular distributions (the polar angles relative to the beam direction,  $\Theta_\gamma$ ) for photons produced in hadronic decays of the  $Z^0$  and converted in the DELPHI detector before the TPC. The photon kinematic range is  $0.2 < E_\gamma < 1 \text{ GeV}$  and the photon polar angle relative to the parent jet direction  $\theta_\gamma > 200 \text{ mrad}$ . The MC data were corrected by the recalibration procedure reducing the difference in material distributions in the RD and the MC and possible pattern recognition biases (see text); b) the relative difference between the RD and corrected MC distributions.

# DELPHI

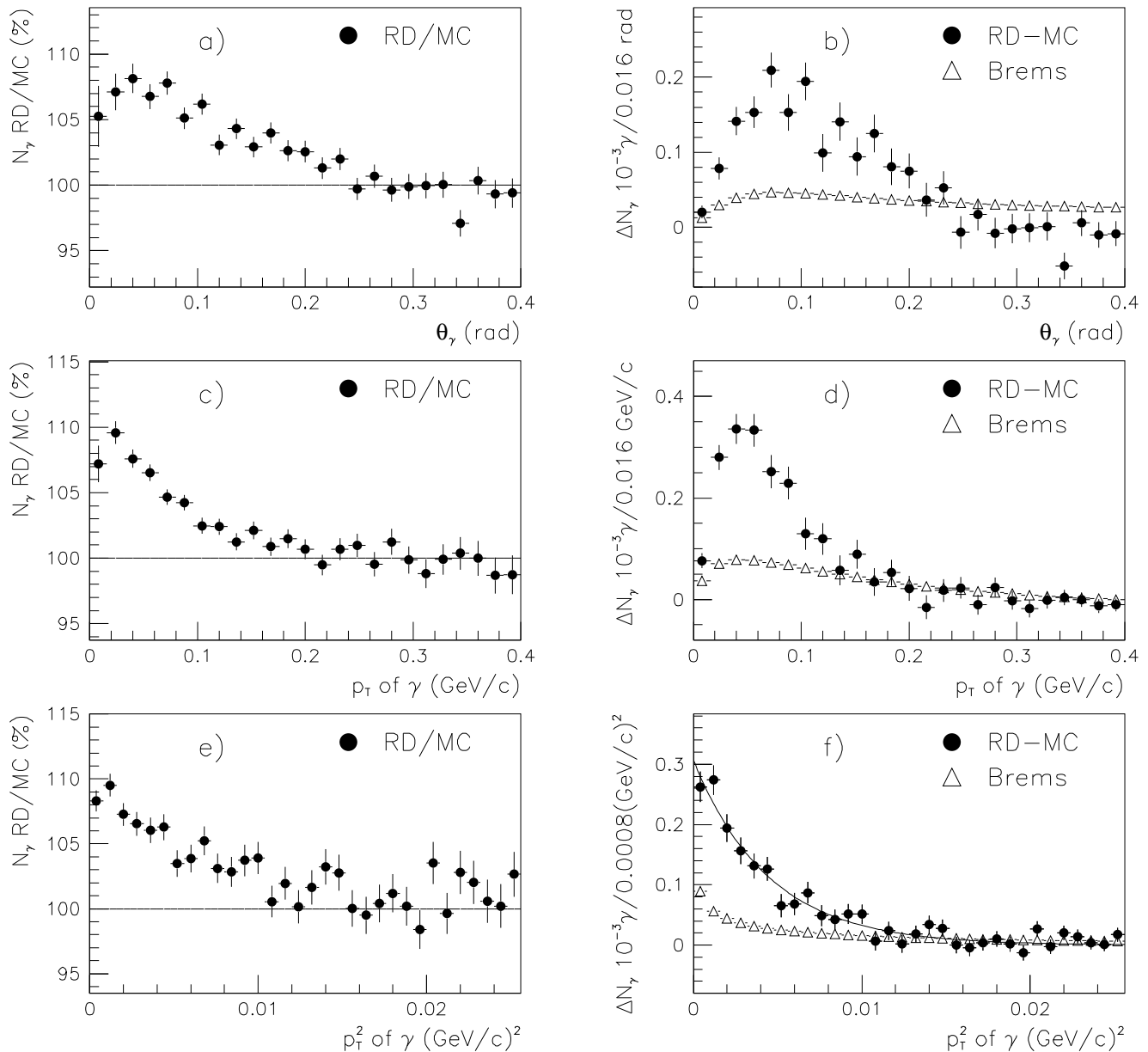


Figure 3: Experimental spectra obtained with the general selection. Left panels: the ratio of the RD and MC distributions for a)  $\theta_\gamma$  (photon polar angle relative to the parent jet direction); c) photon  $p_T$ ; e) photon  $p_T^2$ . Right panels, b), d), f): the difference between the RD and MC distributions for the same variables, respectively. “Brems” corresponds to the inner hadronic bremsstrahlung predictions. The errors are statistical. The curve in fig. 3f) is the fit by an exponential (see text).

# DELPHI

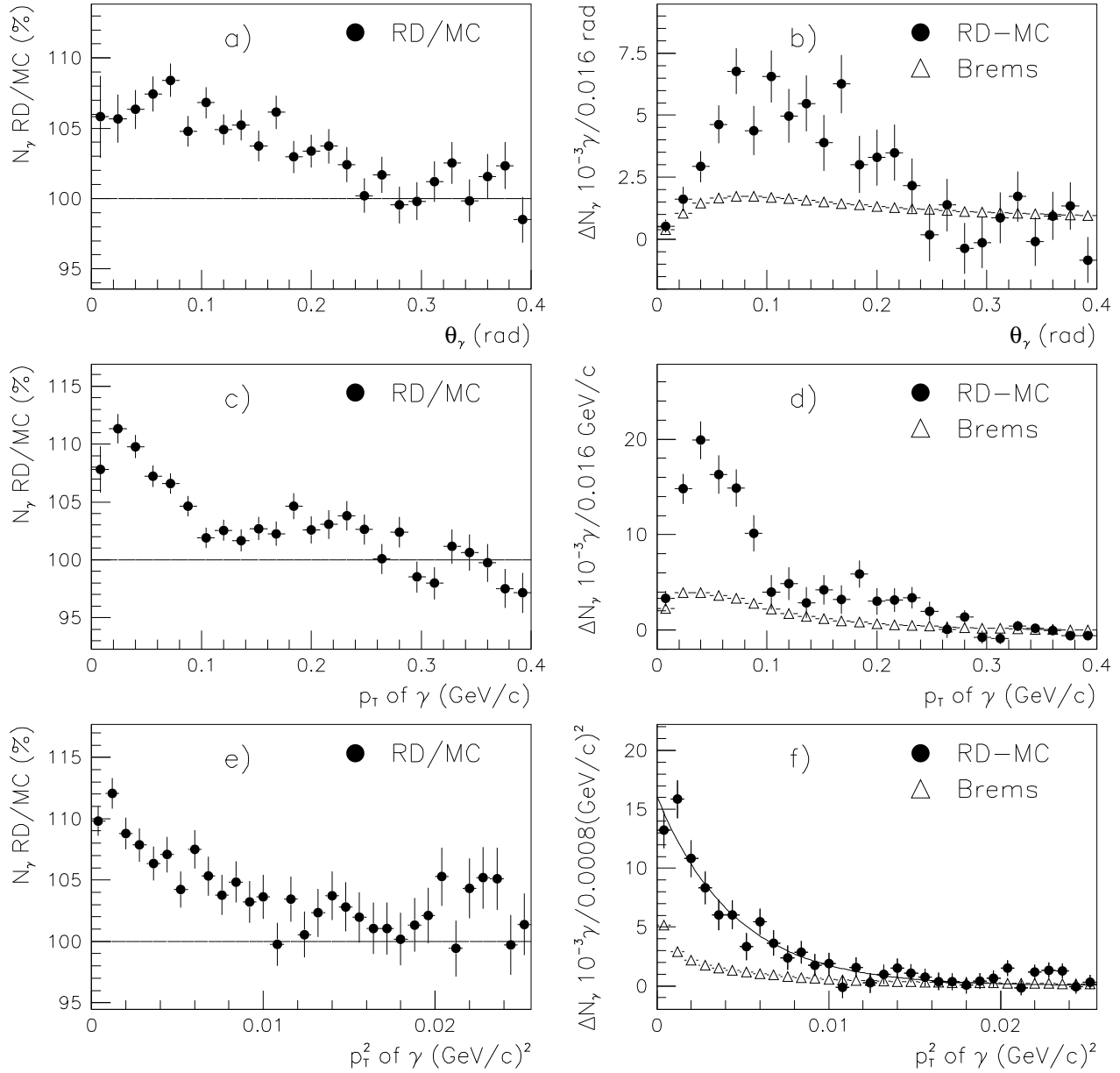


Figure 4: The same as in fig. 3, corrected for the efficiency of photon detection.



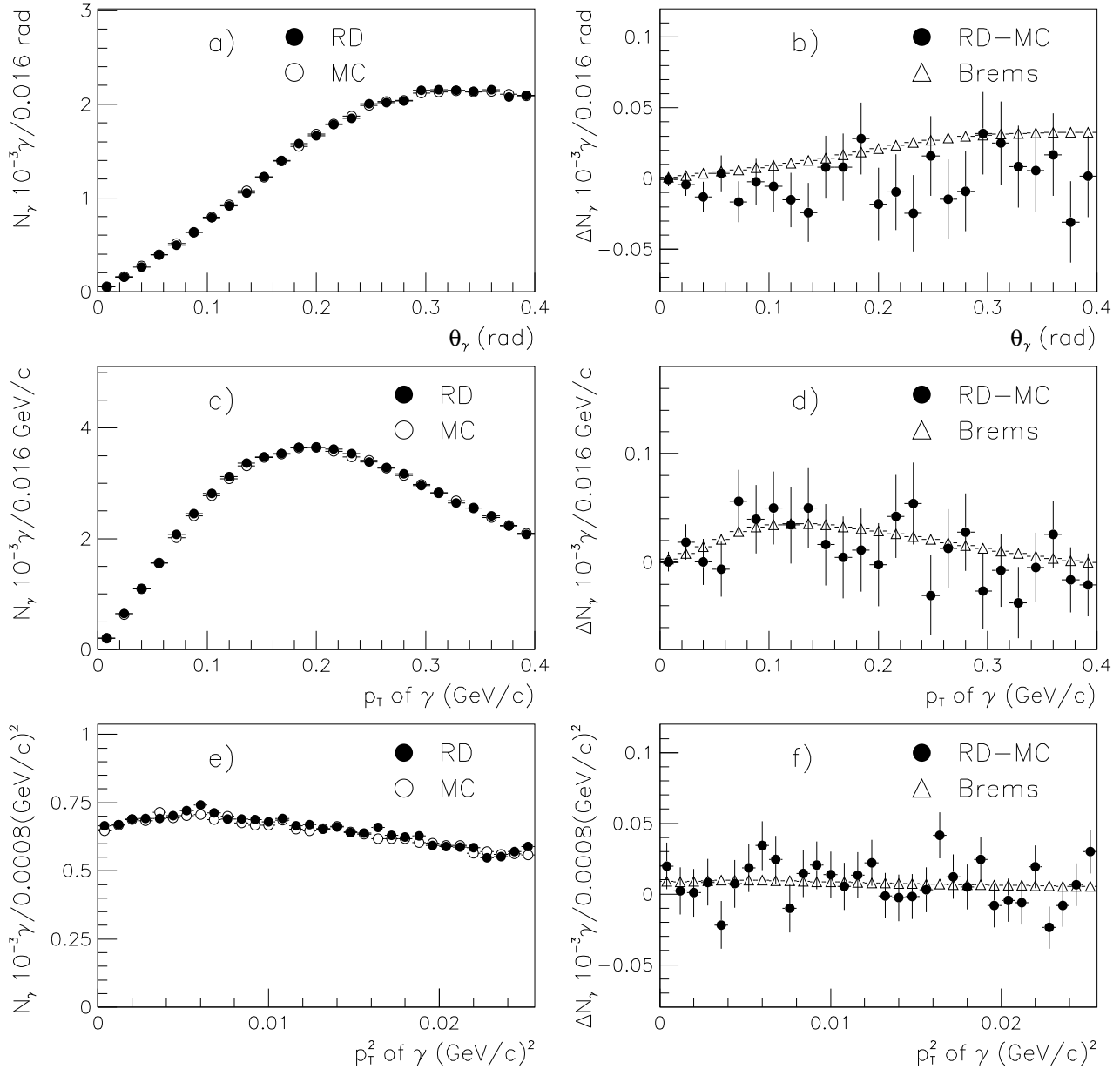


Figure 5: Zero experiment photon distributions. Left panels, a), c), e): the RD and MC  $\theta_\gamma$ ,  $p_T$  and  $p_T^2$  distributions; right panels, b), d), f): the difference between the RD and MC distributions for the same variables together with the bremsstrahlung predictions. The errors are statistical.

# DELPHI

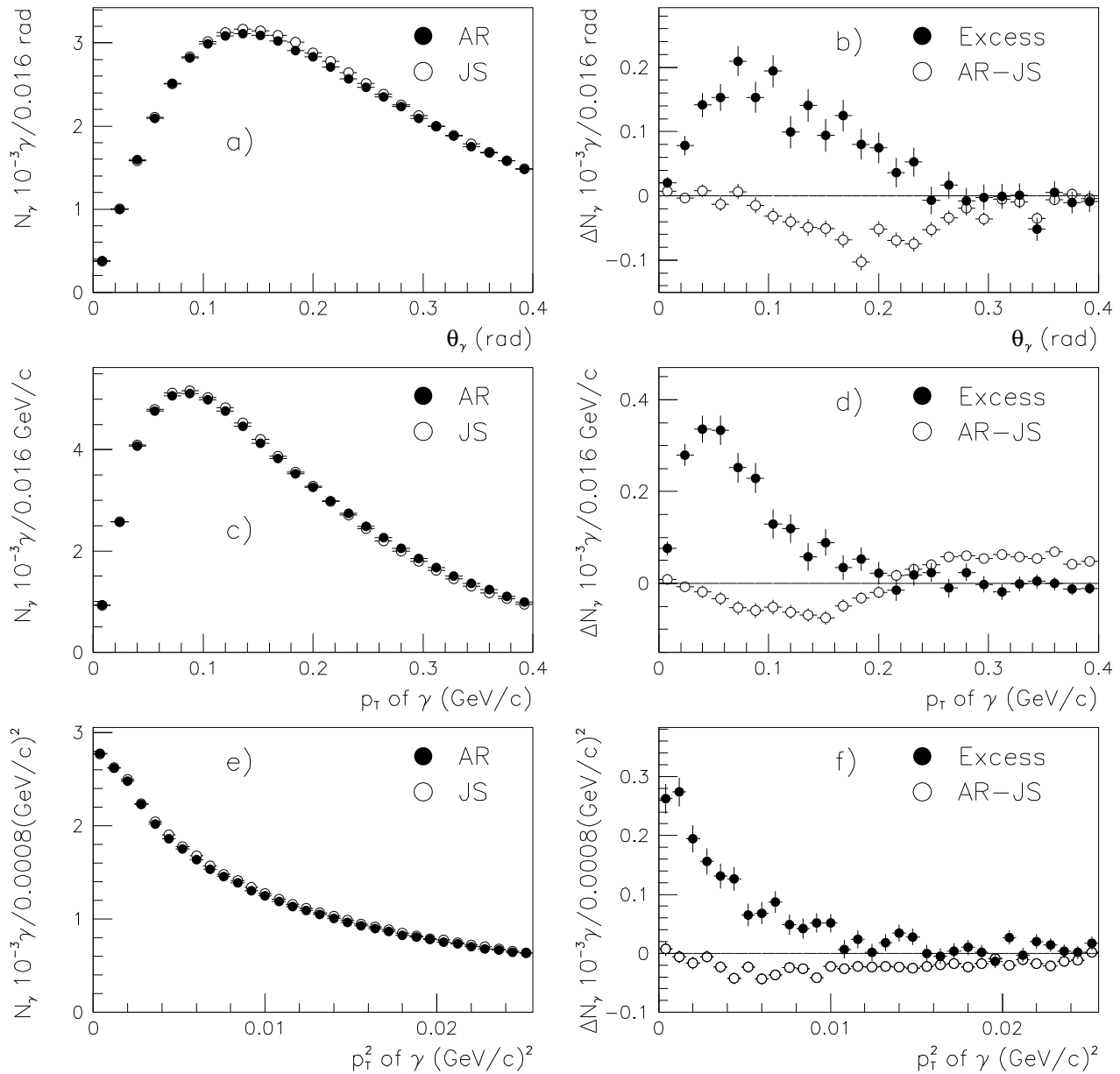


Figure 6: Comparison of the JETSET (JS) and ARIADNE (AR) generators. Left panels, a), c), e): the MC  $\theta_\gamma$ ,  $p_T$  and  $p_T^2$  distributions of photons as produced by JETSET and by ARIADNE. Right panels, b), d), f): the difference between the two MC distributions for the same variables (open circles). The RD-MC distributions from fig. 3 presenting the observed excess are also displayed for comparison. The errors are statistical.

# DELPHI

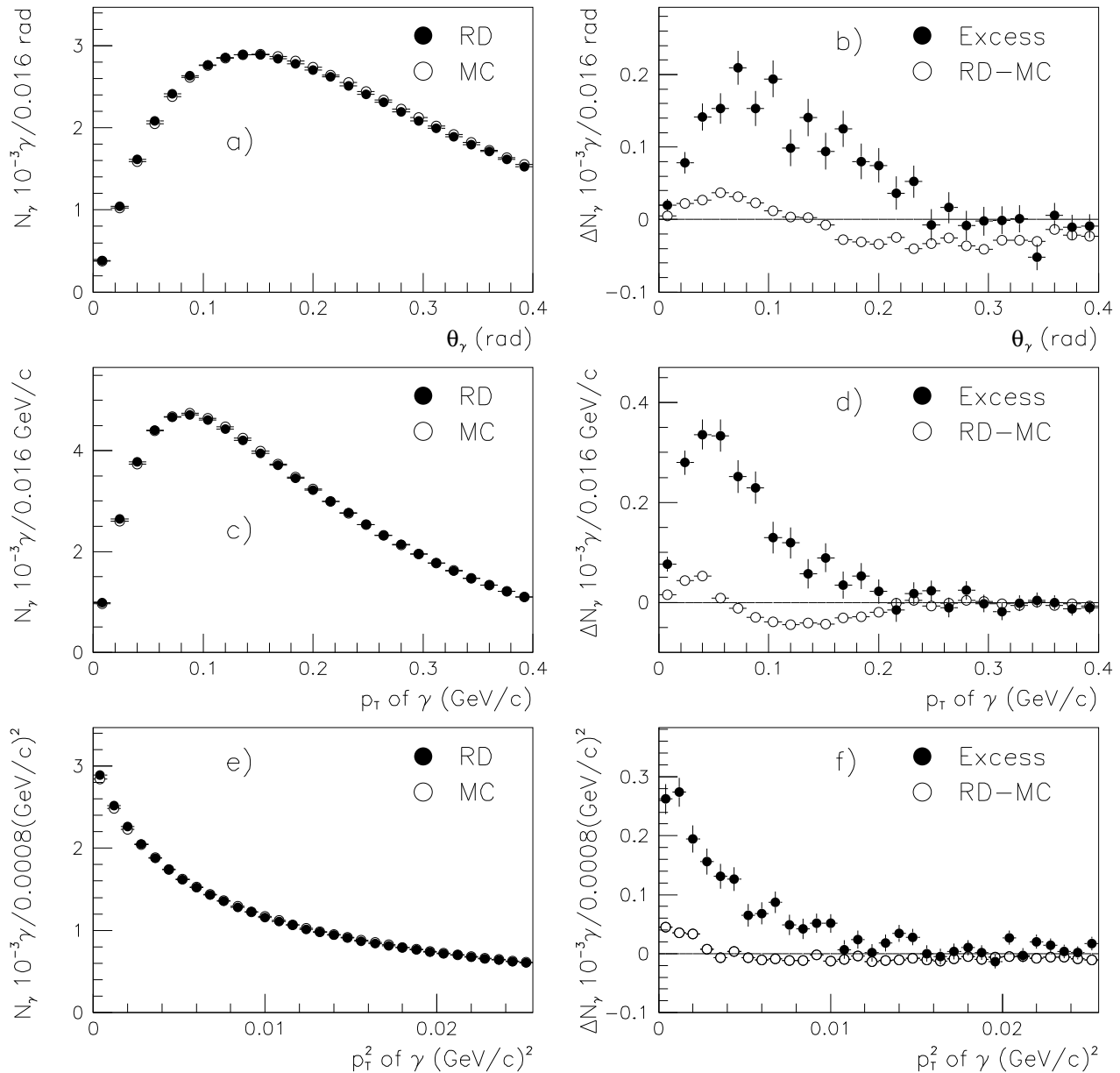


Figure 7: Comparison of the RD and MC distributions of “photons” produced from charged particles (see text, section 6.5). The RD–MC distributions for these “photons” are shown by open circles. The observed excess distributions (RD–MC from fig. 3) are also displayed for comparison. The errors are statistical.

# DELPHI

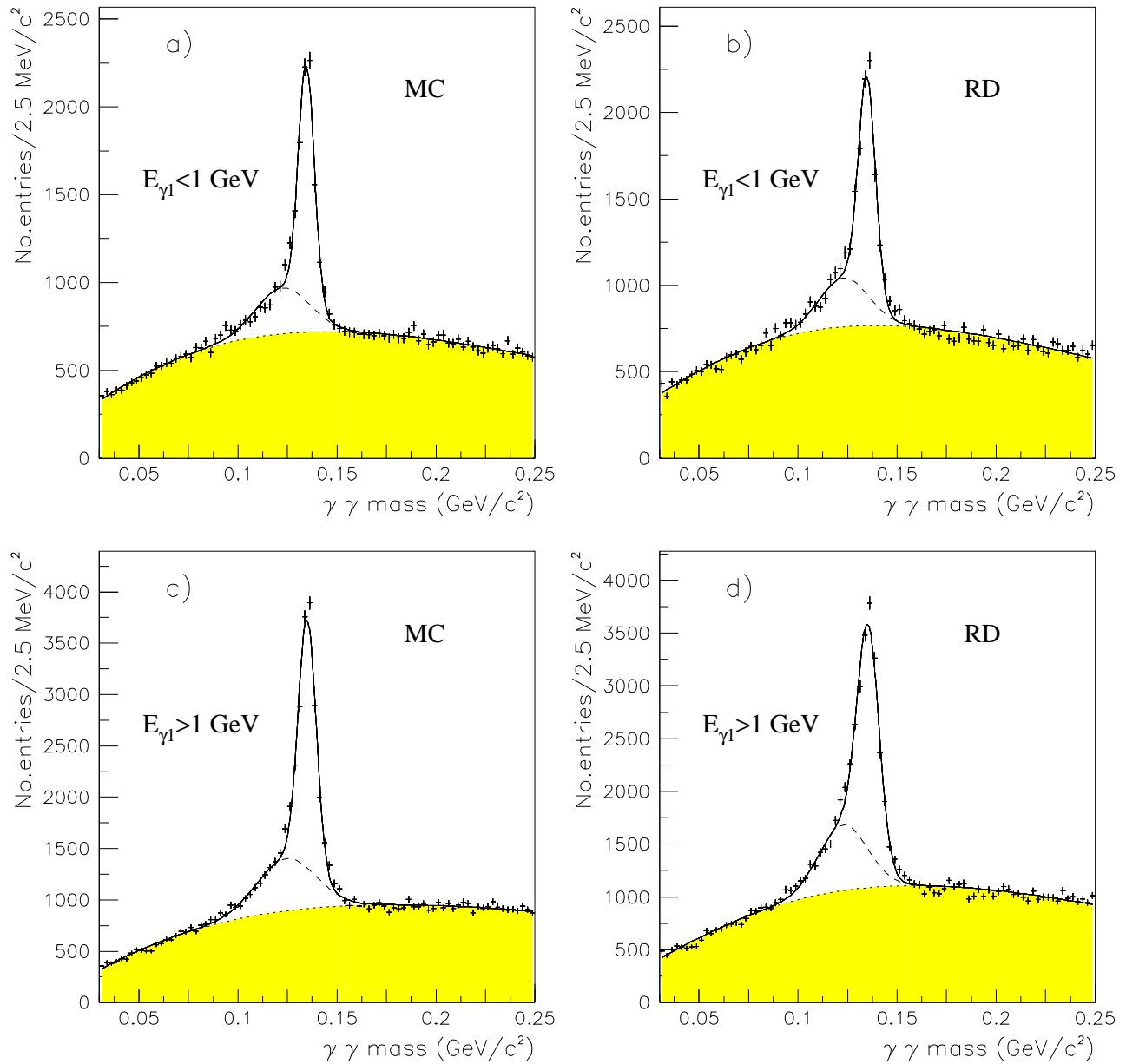


Figure 8: Comparison of the MC and RD  $\gamma\gamma$  mass distributions for the two converted photon combinations. a,b) LE $\times$ HE combination; c,d) HE $\times$ HE combination. The dashed line represents the distortion Gaussian (see text). The errors are statistical. The results of the comparison are given in table 6.

# DELPHI

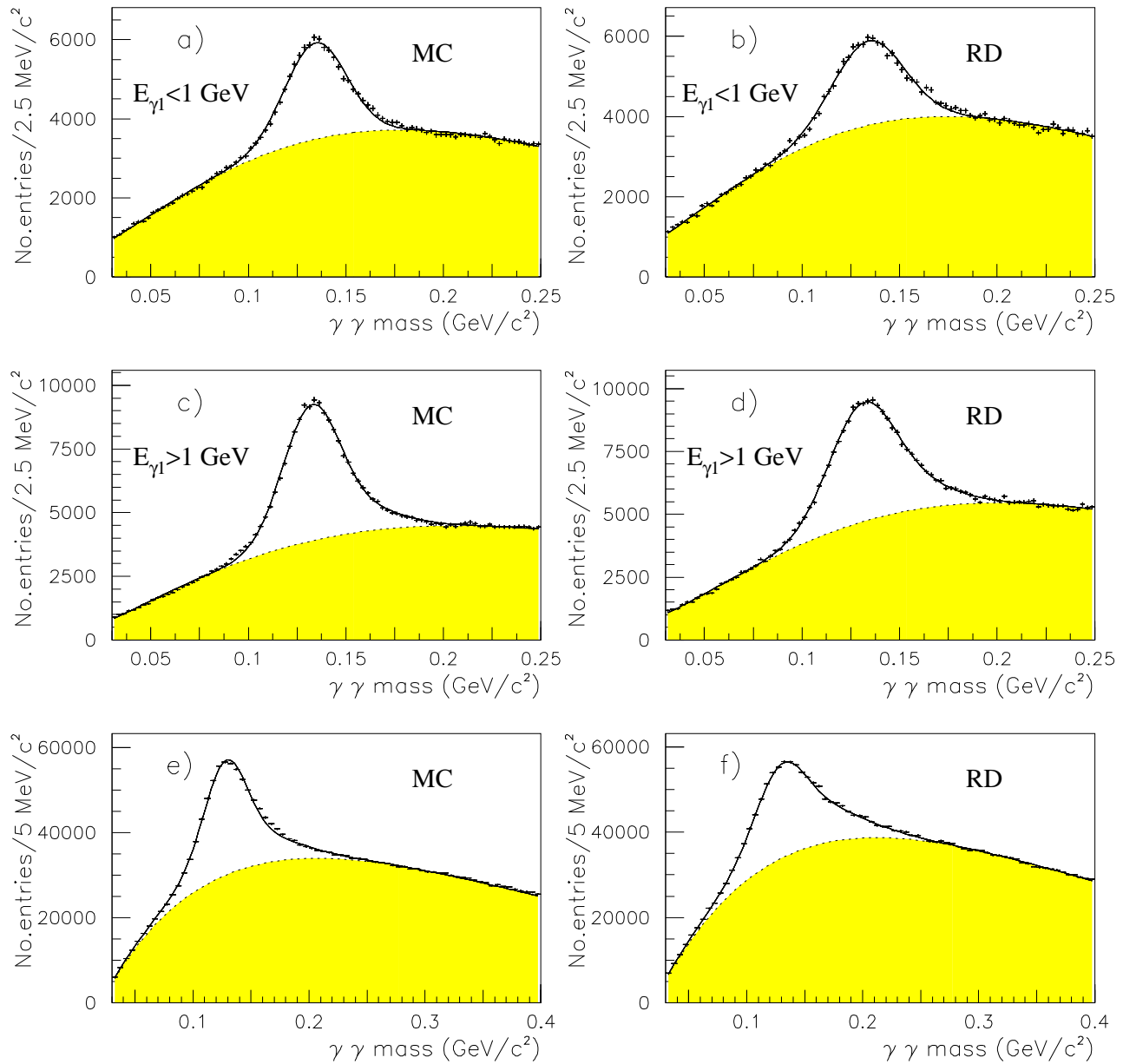


Figure 9: Comparison of the MC and RD  $\gamma\gamma$  mass distributions for converted and high energy HPC photon combinations. a,b) converted LE and HPC combination; c,d) converted HE and HPC combination; e,f) HPC and HPC combination (note the different mass scale for these plots). The errors are statistical. The results of the comparison are given in table 7.